ALTERED BIOMECHANICAL PROPERTIES OF LARGE ARTERIES IN MUSCULAR DYSTROPHY

A Thesis

by

WENDY WATSON DYE

Submitted to the Office of Graduate Studies of
Texas A&M University
in partial fulfillment of the requirements for the degree of

MASTER OF SCIENCE

August 2005

Major Subject: Biomedical Engineering

ALTERED BIOMECHANICAL PROPERTIES OF LARGE ARTERIES IN MUSCULAR DYSTROPHY

A Thesis

by

WENDY WATSON DYE

Submitted to the Office of Graduate Studies of
Texas A&M University
in partial fulfillment of the requirements for the degree of

MASTER OF SCIENCE

Approved by:

Chair of Committee, Jay D. Humphrey
Committee Members, Emily Wilson
John Criscione
Head of Department, Gerard Coté

August 2005

Major Subject: Biomedical Engineering

ABSTRACT

Altered Biomechanical Properties of Large Arteries

in Muscular Dystrophy. (August 2005)

Wendy Watson Dye, B.S., Texas A&M University

Chair of Advisory Committee: Dr. Jay D. Humphrey

Muscular dystrophy is a disease characterized by skeletal muscle weakness and wasting, but little is known of alterations in the vascular system that occur with this disease. The culprit in many muscular dystrophies is a defective dystrophin-glycoprotein complex (DGC). The DGC is a group of transmembrane proteins that connects the cytoskeleton of muscle cells to the extracellular matrix; it plays a role in mechanotransduction and the maintenance of structural integrity of these cells, and includes the proteins dystrophin and sarcoglycan-delta. The absence of these proteins results in severe muscular dystrophies in humans, and thus knockout mice lacking the genes encoding for dystrophin (*mdx* mice) and sarcoglycan-delta (*sgcd-/-* mice) were studied to detect any vascular alterations that occur as a result of a defective DGC. Acute biaxial biomechanical data were obtained through pressure-diameter and axial force-length tests on common carotid arteries of *mdx*, *sgcd-/-*, and wild-type mice in the active and passive smooth muscle state. Functional response to the vasoreactive compounds phenylephrine, carbamylcholine chloride, and sodium nitroprusside was also tested. We found significant biomechanical differences between the knockout and wild-type mouse arteries: the *mdx* and *sgcd-/-* arteries had decreased distensibilities in pressure-diameter tests, with *mdx* arteries also having increased circumferential stresses, and the knockout arteries generated increased axial loads and stresses in the axial force-length tests. The *mdx* and *sgcd-/-* arteries also differed from the wild-type in that their ‘homeostatic’ axial stretch, at which the axial force remains constant

upon pressurization, was significantly decreased. We conclude that the loss of DGC proteins does trigger changes in vascular smooth muscle cells or their interactions with the extracellular matrix, yet that the altered vascular system was able to adapt and function without the DGC. Knowledge of alterations to the vascular system (and adaptations to these changes) of patients with muscular dystrophy could help physicians customize their treatment to extend and enhance their lives, especially as medical advances extend the lifespan of these patients and they begin to suffer from diseases such as hypertension and atherosclerosis that affect the normal aging population.

ACKNOWLEDGEMENTS

This research project was funded through the Muscular Dystrophy Association (MDA) grant #MDA 3681. I would like to acknowledge especially Dr. Rudy Gleason for his instruction and patience in helping me complete my project, and also Dr. Jay Humphrey, Dr. Emily Wilson, and Dr. John Criscione for their encouragement and direction. I would lastly like to thank my husband Jeremy for always being ready and willing to offer advice and assistance for any task that needed to be done.

TABLE OF CONTENTS

LIST OF TABLES

LIST OF FIGURES

FIGURE Page

CHAPTER I

INTRODUCTION

Muscular dystrophies are a broad group of hereditary diseases, characterized primarily by progressive muscle weakness and wasting, that affect both humans and animals. One type of muscular dystrophy that is both severe and common was named Duchenne's muscular dystrophy (DMD) for one of the physicians who first documented the disease in 1868, Guillame-Benjamin-Amand Duchenne. This particular disease was, at the time, called "pseudo-hypertrophic muscular paralysis" because of the pronounced hypertrophic growth and deterioration of function of the lower-limb muscles. The same disease had actually been observed previously and described by the English physicians Edward Meryon, William Little, and Richard Partridge as well as two Italian physicians, Gaetono Conte and L. Gioja.[50] All of the descriptions note that the patients presenting with the disease were males (often brothers) under the age of 20 who developed enlarged but weakened muscles, especially in their lower extremities, and died very young, usually from respiratory failure. Duchenne, who took muscle biopsies from his patients, also described the morphology of the disease. He saw that many muscle fibers in affected patients were either hypertrophic or atrophic with progressive interstitial fibrosis, showing regions of necrosis and regeneration.[43] The English neurologist Sir William Richard Gowers took a special interest in the disease and offered additional conclusions about pseudo-hypertrophic muscular paralysis. He described in detail the unusual way that patients afflicted with the disease were able to maneuver themselves into a standing position, which is now called the "Gowers sign" and is an easily recognizable characteristic for DMD. Gowers also speculated that the disease, manifesting itself predominately in males and often in multiple siblings, was hereditary.

This thesis follows the style of the *Annals of Biomedical Engineering*.

His series of lectures on the disease included this moving description of pseudo-hypertrophic muscular paralysis: and at the

> The disease is one of the most interesting, and at the same time most sad, of all those with which we have to deal: interesting on account of its peculiar features and mysterious nature; sad on account of our powerlessness to influence its course, except in a very slight degree, and on account of the conditions in which it occurs. It is a disease of early life and of early growth. Manifesting itself commonly at the transition from infancy to childhood, it develops with the child's development, grows with his growth, so that every increase in stature means an increase in weakness, and each year takes him a step further on the road to a helpless infirmity and in most cases to an early and inevitable death.[19]

In later years, physicians began to sort out variations of this disease described by Duchenne and Gowers and described them as muscular dystrophies. Becker's muscular dystrophy (BMD) was identified by its similarity but decreased severity to DMD, and different forms such as limb-girdle muscular dystrophy (LGMD) and myotonic muscular dystrophy were described.[52] Techniques in molecular biology refined over the past fifty years enabled scientists to locate the DMD gene locus on the short arm of the human X chromosome and clone it without knowing the protein product.[35] The gene was found to be very large, comprising about 1/1000 of the total human genome, and thereby susceptible to spontaneous mutations.[37] Then, in 1987, the protein product of the known DMD locus was identified and named dystrophin.[23] Soon thereafter, scientists found that human DMD is caused predominately by deletions in the dystrophin gene (although rearrangements and point mutations are also common) that result in a truncated and nonfunctional dystrophin protein. The molecular basis of other muscular dystrophies, especially those linked to proteins associated with dystrophin in a dystrophin-glycoprotein complex (DGC), also began to be examined. This complex consists of a series of interacting proteins that provides a crucial link between the actin cytoskeleton of muscle cells and laminin in the extracellular matrix. The DGC includes dystrophin, the dystroglycans, the sarcoglycans, sarcospan, dystrobrevin, and the syntrophins (Figure 1).[8] BMD was found to be

caused by dystrophin that is either truncated or reduced in amount but still functional, and severe forms of LGMD were found to be caused by defects in the sarcoglycan genes. LGMD is characterized clinically by symmetrical weakening of the pelvic, scapular, and trunk muscles along with elevated serum creatine kinase levels and a degeneration-regeneration muscle cycle; this disease can be as devastating as DMD in some cases.[13]

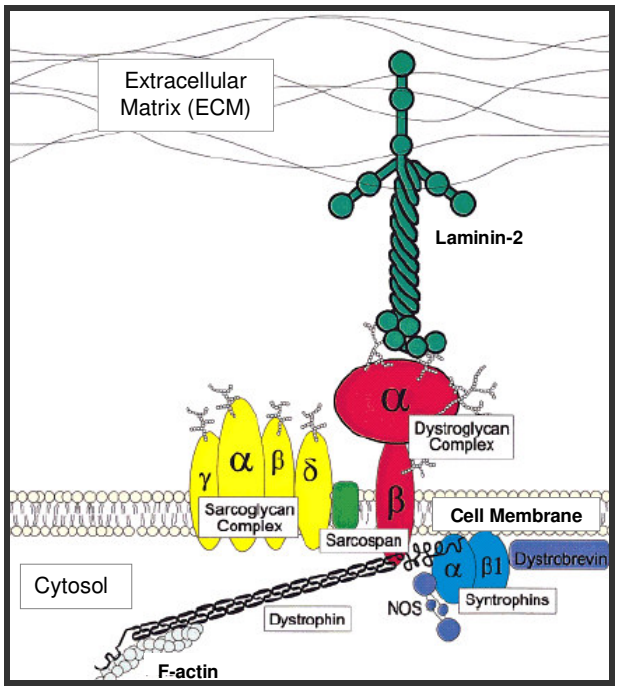

Figure 1: The dystrophin-glycoprotein complex. This group of proteins connects the intracellular cytoskeleton of muscle cells to laminin in the extracellular matrix (figure adapted from Cohn and Campbell, 2000).[8]

Researchers simultaneously were analyzing the genome of the *mdx* mouse, which has an X-linked muscular dystrophy and was a potential animal model for DMD. They showed that a single point mutation in the murine dystrophin gene, homologous to the human DMD locus, causes premature termination of protein translation, resulting in an absence of dystrophin.[45] This brings us to today, when much of the current research being conducted on DMD now utilizes the *mdx* mouse and other mouse knockout models to assay the consequences of the absence of various DGC proteins.

When referring to the *mdx* mouse as a model for human DMD, the vast difference in the disease phenotype between the mouse and human should be discussed. In people afflicted with DMD, muscle cells progressively degenerate and become fibrotic (as collagenous and adipose tissue replaces the muscle fibers), [42] and motility and life-span are drastically decreased (most patients are wheelchair bound by the age of 11 and do not live beyond the age of 30).[23] *mdx* mice, on the other hand, display no overt muscle weakness and have only a slightly reduced life span.[11] Also, when researchers examined the histopathology of the muscles of *mdx* mice over time, they found that there is a period of muscle degeneration, with invasion of neutrophils and macrophages, followed by a period of regeneration in which satellite cells invade and form a new population of muscle fibers that have characteristic internal nuclei. For example, degenerating fibers were visible in the extensor digitorum longus muscle at 2 weeks of age, but the maximum degenerative/regenerative activity occurred at 3-4 weeks. At 12 weeks of age, only 20% of the fiber area of the muscle was composed of the original fibers. At 26 weeks of age, 95% of the fiber area was occupied by regenerated fibers with internal nuclei and even so, the process of degeneration and regeneration was still occurring.[6] A histopathological study later verified these results, but showed further that in older *mdx* mice (12-24 months of age), degeneration continues while regeneration declines progressively, resulting in muscle atrophy

and fibrosis.[39] Systemic serum levels of creatine phosphokinase (CPK), which is an indicator of muscular distress, follow a similar time-course. CPK levels increase 10-fold from normal baseline levels at 3-5 weeks of age in the *mdx* mouse and remain elevated until about 29 weeks of age, when they normalize.[11]

Another characteristic of *mdx* mouse muscle is the functional compensation of a dystrophin-related protein named utrophin. Utrophin has a structure similar to dystrophin, lacking a portion of the rod domain but possessing an actin-binding domain on its amino-terminus and a cysteine-rich domain on its carboxyl-terminus.[49] In normal human and mouse muscle, this protein is found primarily at the neuromuscular junction. In human DMD and *mdx* mouse muscle, utrophin is not only found throughout the sarcolemma of small-caliber skeletal muscles and cardiac muscle, it also associates with the DGC there.[31] An interesting finding is that utrophin is present in higher concentrations during fetal development of the *mdx* mouse and is reduced to adult levels by the third week after birth. The reduction of utrophin levels coincides with the greatest incidence of muscle degeneration, and the regenerating fibers that begin appearing label intensely for utrophin.[27] An additional finding is that mice genetically altered to lack the genes dystrophin and utrophin display a severe muscle wasting phenotype from early in life and also have a shortened life span (about 20 weeks). These double knockout mice seem to have a disease with symptoms equivalent to human DMD,[12] which indicates with the other studies that utrophin has a role (perhaps particularly in development) in establishing and maintaining functional muscle in the *mdx* mouse. An extra note is that utrophin was also found with immunohistochemistry to be strongly expressed in vascular smooth muscle cells.[16]

The *mdx* mouse is still being used to pursue treatments for DMD such as gene repair, stimulation of skeletal muscle regeneration, and replacement with stem cells.[5] Research efforts are also focused on expanding the body of knowledge on what dystrophin and the DGC actually

do in muscle cells. Although it has been studied for nearly 20 years, the exact physiological function of the dystrophin protein and the DGC is unknown in any muscle type.

Some components of the DGC seem to have a primarily structural role in the complex. Dystrophin is known to have such a role in establishing the other members of the DGC on the muscle membrane. Dystroglycan, a protein product of one gene that is eventually cleaved into α and β subunits, is the physical connector spanning the membrane of the cell. β-dystroglycan interacts with dystrophin at its carboxyl-terminus inside the cell, extends across the cellular membrane, and binds to α-dystroglycan extracellularly.[44] α-Dystroglycan then binds laminin specifically in a calcium- and ionic-dependent manner.[14] The dystroglycans are also associated with the sarcoglycans,[53] which are transmembrane glycoproteins of which there are six different types. The combination of sarcoglycan proteins varies for the different muscle types. Skeletal and cardiac muscle possess α-, β-, δ-, and γ-sarcoglycan. In the vascular smooth muscle cells, ε-sarcoglycan replaces α-sarcoglycan (the two are nearly homologous type I transmembrane proteins) and ζ-sarcoglycan takes the place of γ-sarcoglycan (both highly related type II transmembrane proteins) while β- and δ-sarcoglycan remain.[37] The loss of any of the sarcoglycan proteins causes the sarcoglycan subcomplex to be disrupted, with the other three sarcoglycan proteins being reduced or absent at the cell membrane.

Other proteins of the DGC seem to function as signaling rather than structural proteins. One such member is syntrophin, a 58-kDa protein with three different isoforms (α, β_1, and β_2) that localizes to the carboxyl-terminus of dystrophin.[1] Syntrophin has been found to bind to dystrobrevin, Grb2, calmodulin, PIP2, and neuronal nitric oxide synthase (nNOS); some of these proteins are involved in signaling pathways.[4] nNOS is of particular interest in this study, as it is part of the DGC in skeletal and vascular smooth muscle where it functions to attenuate vasoconstriction of the vascular smooth muscle.[47]

Studies of the consequences of the absence of dystrophin and the DGC have focused on two main potential malfunctions. One is the increased susceptibility of skeletal muscle to fatigue due to the mechanical strains of muscle contraction (shown in *mdx* mice).[18] The other is a disruption of intracellular calcium homeostasis in muscle fibers. One study of dystrophin deficient skeletal muscle in *mdx* mice tried to discern if the primary malfunction in dystrophin-deficient muscle is the weakness of the sarcolemma or the altered state of the Ca^{2+} ion channel, that is, an increase in membrane permeability to the calcium ion. They postulated that if the former is the primary defect, then membrane damage would correlate directly to the magnitude of the membrane stress for each contraction. In contrast, if the Ca^{2+} ion channel state is the primary defect, then damage should be due to repeated activation of the muscle that increases Ca^{2+} load.[41] One result was that there was no significant difference between the dye-containing (indicating damage) muscle fibers in *mdx* mice in two tests in which identical isometric contractions are applied but the number of activations is increased 10-fold in one case. On the other hand, there was a significant correlation for both wild-type and *mdx* mice between the peak force (normalized for muscle cross-sectional area) and the percentage of dye-containing fibers. The conclusion of the study was that the extent of damage in dystrophic muscle is significantly higher for higher amounts of stress, which may overload the regenerative capacity of the muscle and leave it permanently injured. In further defense of the conclusion that dystrophin-deficient muscle is more susceptible to mechanical damage, it has been found that dystrophin expression in healthy skeletal muscle is concentrated at regions known to experience the highest levels of axially and radially transmitted mechanical stress, such as the attachment points between the sarcolemma and sarcomere.[42] It can thereby be postulated that under normal conditions, dystrophin and the remainder of the DGC have the primary role of redistributing the mechanical stresses involved in contraction throughout the cell and to the extracellular matrix to maintain the

structural integrity of muscle cells. This is thought to be accomplished as dystrophin, along with intact sarcoglycan and dystroglycan complexes, acts as a link and/or a spring to relieve local stresses imposed on cell membranes by distributing them throughout the cell,[38] thus protecting cells from rupture during repeated contraction and relaxation.[20]

The current hypothesis that dystrophin and the DGC have a mechanical role in protecting muscle cells from injury during contraction has interesting implications for the vascular system of veins, arteries, and capillaries, which is largely composed of smooth muscle cells, embedded in an abundant extracellular matrix, that are constantly subjected to axial and circumferential stresses and endothelial cells subjected to shear stresses (dystrophin is known to be present in both vascular smooth muscle cells and endothelial cells).[28] Some observations have been made on the state of the vasculature in humans with muscular dystrophies. Early studies of DMD outlined a theory of disease progression that involved a defect in the microcirculation, and irregularities in the microcirculation have been reported in cases of muscular dystrophy. For example, a number of abnormalities were apparent in capillary beds of the biceps brachii of very young DMD patients in the preclinical stages of the disease. Electron microscopy revealed swollen endothelial cells in ~30% of the small vessels, increased capillary wall and endothelial cell areas, and thicker basement membrane around the vessels.[33] Also, one study of over 100 patients undergoing surgery to correct spinal scoliosis included a large subset of young patients diagnosed with DMD ($n = 48$) as well as patients with spinal muscular atrophy and others without muscular dystrophy; the study examined the values for estimated blood volume and blood loss for the patients during surgery. The estimated blood volumes were similar between groups, but the DMD patients had a significantly greater estimated blood loss even though the duration of surgery for all groups was similar.[36] It has also been reported that human patients

with Becker's muscular dystrophy have a higher local blood flow rate in the tibialis anterior muscle than normal subjects, as measured by the ^{133}Xenon clearance method.[32]

More recently, it has been shown that *mdx* mouse arteries do not have a normal response to increased flow rates. In one study, isolated carotid and mesenteric arteries were both shown to have significantly attenuated vasodilation in response to acute increased flow when compared to wild-type arteries.[28] The structure of the vessels seemed to be somewhat different also, as the wall-to-lumen ratio was significantly increased in *mdx* arteries and the calculated compliance and distensibility were decreased. Yet, in many other aspects there were no significant differences between *mdx* and wild-type arteries, such as diameter changes in response to pressure steps (in active and passive smooth muscle states), arterial wall thickness, dilation in response to acetylcholine and sodium nitroprusside, contraction in response to calcium, potassium chloride (KCl) or phenylephrine, mean arterial pressure, and body weight. A follow-up study[29] examined the effects of ligations to various branches of the mesenteric arterial system in order to create high flow and low flow situations that should force arterial remodeling. It was found that an increase in blood flow did not induce outward remodeling in the *mdx* mesenteric high flow arteries as it did in the wild-type mouse. Another result was that endothelial nitric oxide synthase (eNOS) expression was not significantly different in high-flow as compared to normal-flow *mdx* arteries, whereas there was a significant increase in eNOS expression between those two groups of wild-type arteries. A later study[30] showed that arteriolar density measured in the right ventricle and in gracilis skeletal muscle is reduced in *mdx* mice as compared to wild-type. Other vascular alterations are present in mice that do not express one of the sarcoglycans, sarcoglycan-delta. These *sgcd-/-* mice have been shown to develop cardiomyopathy as well as irregularities in the coronary vessels such as vascular constrictions and reduced lumen size.[10]

In summary, mice with protein deficiencies that disable the DGC, namely the lack of dystrophin or sarcoglycan-delta, have abnormalities of their vascular systems and are also disease models for the severe human muscular dystrophies DMD/BMD (caused by absent or reduced levels of functional dystrophin) and LGMD (caused by the absence of sarcoglycan-delta). It is therefore constructive to study the vasculature of these mouse models and report any abnormalities to equip physicians to effectively treat disorders in patients with DMD, LGMD, and other muscular dystrophies. Our research seeks to characterize the inherent biomechanical properties of the carotid arteries from *mdx* and *sgcd-/-* mice as compared to wild-type mice of the same strain. Specifically, we attempted to meet two specific aims. Our first aim was to conduct mechanical and functional tests on arteries from the three mouse types *in vitro*. Our second aim was to analyze the unloaded dimensions, pressure-diameter data, force-length data, and axial and circumferential stress-strain data from tested arteries (that displayed smooth muscle and endothelial function) to make comparisons between mouse genotypes. We also planned to preserve tissue from tested and untested arteries in order to conduct RNA and protein analysis. The next section of this thesis will describe in detail the fulfillment of these aims that allowed us to compare carotid arteries from wild-type, *sgcd-/-*, and *mdx* mice to try to determine any biomechanical differences that may exist between the three groups.

The ultimate goal of this study is to equip physicians to effectively treat disorders in patients with muscular dystrophy. Current muscular dystrophy research efforts are focused on providing a better and longer life for patients with the disease. But, as DMD patients with better medical treatment live longer, there is concern that alterations in the vascular system could cause individuals with muscular dystrophy to be more susceptible to common vascular diseases such as hypertension and atherosclerosis that affect many aging Americans. A better understanding of the effect of muscular dystrophy on the vascular system may enable physicians to tailor

treatment for muscular dystrophy patients with vascular complications. In addition, our examination of the effects of muscular dystrophy on the vascular system will further the body of knowledge on the nature and mechanism of the disease.

CHAPTER II

BIOMECHANICAL TESTING TO DEDUCE PROPERTIES OF MURINE CAROTID ARTERIES MISSING PROTEINS ASSOCIATED WITH MUSCULAR DYSTROPHY

Introduction

Muscular dystrophy is caused by genetic defects of the components of the dystrophin-glycoprotein complex (DGC). This complex links the actin cytoskeleton of muscle cells to the adjacent extracellular matrix, and is responsible for redistributing stresses on muscle cells to maintain structural integrity during contraction and relaxation. The absence of DGC proteins could have important implications for the vascular system, which is composed largely of an abundant extracellular matrix (ECM) with embedded smooth muscle cells (SMCs) that possess the DGC and are constantly subjected to axial and circumferential stresses. It is possible that the biomechanical properties of the vasculature are altered in individuals with muscular dystrophies, and these alterations could contribute to the progression of the skeletal muscle disease as well as cardiovascular, neurovascular, and renovascular diseases.

The acute biomechanical and functional properties of dystrophin-deficient (*mdx*) mice and sarcoglycan-delta-deficient (*sgcd-/-*) mice were compared to those of wild-type controls to elucidate any muscular dystrophy-related abnormalities. To this end, a computer-controlled perfused organ-culture device[15] was used to measure and independently control pressure, axial stretch (or force), and luminal flow while measuring the outer diameter of the vessel by collecting and processing images from a video-microscope. Values for these and other variables were collected at a user-defined rate and written to a computer file for off-line analysis. Analysis of the data collected through these methods revealed significant alterations in the carotid arteries

of mice lacking proteins associated with severe human muscular dystrophies.

Methods

Arterial Isolation and Setup in Biaxial Testing Device

Wild-type and *mdx* mice were ordered from Jackson Laboratories (Bar Harbor, Maine), while breeding pairs of *sgcd-/-* mice were given by Kevin Campbell (University of Iowa) and their offspring used for experiments. All animals were maintained by the Texas A&M University Laboratory Animals Resources and Research (LARR) program and were used in accordance with the University Lab Animal Care Committee (ULACC) guidelines. Wild-type (n = 6), *mdx* barrier AX6 (n = 5), and *sgcd-/-* (n = 6) male C57BL/6J mice, between 8 and 12 weeks old, were euthanized with a lethal injection of sodium pentobarbital (50mg/kg IP) containing heparin (1000-unit/kg IP) and left and right common carotid arteries were isolated. Left arteries were placed in warm Dulbecco's modified Eagle's medium (DMEM, Invitrogen, Inc.), supplemented with 10% heat-inactivated fetal bovine serum (HI-FBS, Hyclone) as well as 1000 units/L penicillin and 1000 g/L streptomycin (P/S, Invitrogen, Inc.), and mounted on perfusion glass cannulae at both extremities using 6-0 suture.

The cannulated left arteries were placed in a bath of fresh, warm DMEM supplemented as above within the incubator chamber of the testing device. Flow was initiated intraluminally and adventitially from two reservoirs of supplemented DMEM. A load cell was attached to the distal cannula and the vessel was imaged. Once an image was obtained, measurements in the unloaded configuration (with mean pressure P = 0 mmHg and axial load f = 0 g) were obtained. The unloaded diameter D of the vessel was noted, and the overall axial length where the vessel just begins to bend was measured as described by Gleason et al.[15] and called the unloaded length L. After the unloaded configuration measurement, the vessel was stretched axially and

pressurized slowly until brought up to *in vivo* conditions (axial stretch λ_z = 1.8 times the unloaded length, P = 100 mmHg, mean intraluminal flow Q = 0.05 ml/min, and temperature T between 32-38°C) after which it remained for 30 minutes. After this equilibration period, the intraluminal flow was stopped and the vessel was subjected to two cycles of preconditioning, at λ_z = 1.95 with P cycled from 0 to 160 mmHg.

Mechanical and Functional Testing

Mechanical testing consisted of two parts, pressure-diameter (*P-d*) and force-length (*f-* ℓ) tests. Before the first *P-d* test, the vessel was depressurized and unloaded to λ_z = 1.0 to verify the unloaded length and diameter. If necessary, a new unloaded length was entered at this point and the axial load zeroed again; reinitializing the system allowed the remainder of the axial stretch data to be based on the new unloaded length. For *P-d* tests, the vessel was stretched to various axial extensions λ_z = 1.60, 1.80, and 1.95 and held while P was cycled from 0 to 160 mmHg. The pressure cycle at each stretch was repeated three times. For *f-*ℓ tests, the vessel was maintained at pressures of P = 60, 100, and 140 mmHg. As the pressure was held constant, λ_z was decreased until the vessel bent and increased up to λ_z = 1.95 twice. At the conclusion of both *P-d* and *f-*ℓ tests, the vessel was depressurized to P = 0 mmHg and unloaded to λ_z = 1.0; the unloaded values L and D were verified, and the axial force value, f, was zeroed again. Lastly, inner and outer diameters were measured by manually adjusting video-calipers in the following 10 different configurations: P = 0 mmHg and λ_z = 1.0, 1.2, 1.4 and 1.65; P = 40 and λ_z = 1.4, 1.65, and 1.8; P = 80 mmHg and λ_z = 1.65 and 1.8; and P = 100 mmHg and λ_z = 1.8.

The vessel was then brought up to λ_z =1.65 and P = 80 mmHg (without flow) for 15 minutes to equilibrate for the function test. At the end of this second equilibration period, the adventitial flow was stopped, and 150 µl of a different agonist was added to the bath every fifteen minutes. The first agonist was phenylephrine (PE) at a concentration of 10^{-3} M (which

diluted to ~10^{-5} M in the bath), which tests for contractile ability of the smooth muscle cells. The next agonist (after 15 minutes) was carbamylcholine chloride (CCh) at a concentration of 10^{-3} M (which diluted to ~10^{-5} M in the bath), which tests for endothelial-dependent smooth muscle cell relaxation. Next, sodium nitroprusside (SNP) was used at a concentration of 10^{-2} M (which diluted to ~10^{-4} M in the bath) to induce endothelial-independent smooth muscle dilation. Finally, after another 15 minutes, the bath was emptied and refilled with warm Hank's Balanced Salt Solution (HBSS, Invitrogen, Inc.) without calcium and magnesium, but with 2 mM EGTA and 10μM SNP to completely relax the smooth muscle cells and the diameter was recorded until it stabilized. We conducted the mechanical tests again with the vessel in the calcium-free HBSS with EGTA to obtain data in a passive smooth muscle state. The *P-d* and *f-ℓ* tests were repeated as described above, the only difference being that two pressure cycles, instead of three, performed at each axial stretch.

Histochemistry

After mechanical and functional testing, the left common carotid arteries were unloaded, removed from the device, and fixed in 4% paraformaldehyde for 1 hour. The arteries were then immersed in a cryoprotectant (30% sucrose) overnight. Next, the arteries were mounted in OCT medium (Tissue Tek) in isopentane cooled with liquid nitrogen, stored at -20°C, and cut into 7 μm sections. Sections of tested arteries for each type were therefore available for future immunohistochemical analysis. The non-tested, right common carotid arteries for each mouse, as well as the thoracic portion of the aorta for a few mice of each genotype, were flash-frozen in liquid nitrogen and stored at -80°C until homogenized for future isolation and analysis of RNA and protein.

Data Analysis

We selected functional vessels for analysis as quantified by at least 30% contraction of

the vessel in response to PE (as compared to the final passive diameter of the vessel in calcium-free HBSS) and at least 15% dilation (from the contraction caused by PE) in response to CCh. Axial force, axial stretch, pressure, and outer diameter data were collected for each vessel at 4 Hz during all tests–active and passive mechanical tests and the functional test. The inner and outer diameters measured at 10 different configurations allowed us to calculate the volume of the vessel wall as

$$V = \pi(b^2 - a^2)\lambda\,, \tag{1}$$

where a is the inner radius and b the outer radius; the 10 different volume values were averaged to give $\overline{V}$. Assuming incompressibility, this mean volume and the outer diameter values allowed the luminal radius a and wall thickness h to be computed at all states using the following formulae:

$$a = \sqrt{b^2 - V/(\pi\lambda)}\,, \tag{2}$$

$$h = (b - a)\,. \tag{3}$$

This, in turn, allowed us to calculate the mean axial and circumferential Cauchy stress (σ_z and σ_θ, respectively) at every test-point, namely

$$\sigma_z = \frac{f}{\pi(b^2 - a^2)}, \tag{4}$$

$$\sigma_\vartheta = \frac{Pa}{h}\,. \tag{5}$$

The axial stretch ratio was calculated as

$$\lambda_z = \ell/L\,, \tag{6}$$

whereas the circumferential stretch ratio was calculated using mid-wall radii:

$$\lambda_\theta = r_{mid}/R_{mid}\,. \tag{7}$$

The current mid-wall radius r_{mid} was calculated as

$$r_{mid} = (a+b)/2, \quad (8)$$

while the unloaded mid-wall radius R_{mid} was calculated as

$$R_{mid} = (A+B)/2 \quad (9)$$

where B is the outer radius in the unloaded configuration (half of the unloaded diameter D) and A can be calculated from wall volume. The inner and outer radii, wall thickness, axial and circumferential stresses and stretches can thus be calculated at every test-point using the unloaded configuration measured prior to that test. By interpolating between test-points, the loaded dimensions, axial force, and axial and circumferential stresses were analyzed using one-factor analysis of variance (ANOVA) for $p < 0.05$, with means separation using Bonferroni's post-hoc test. The body weights of the mice as well as the mean wall volumes and unloaded dimensions of the arteries were similarly analyzed for $p < 0.05$. For the *P-d* test, the outer diameter and axial force were compared between pressures of 2 and 140 mmHg, and the circumferential stretch was compared for circumferential stretches between 0.5 and 1.4 (these ranges of independent variables were common for all vessels of the three genotypes, thus enabling statistical comparison). For the *f-ℓ* test, axial force and axial stress were compared from the lowest common axial stretch up to an axial stretch of 1.95.

Another comparison from the *f-ℓ* test was made. It is known that blood vessels are extended far beyond their unloaded length *in vivo*, and also that at the *in vivo* axial length or axial stretch ($\lambda_{z\ in\ vivo}$, the *in vivo* length normalized to the unloaded length) the axial force tends to remain constant over a range of pressures.[24] One way to discern the *in vivo* axial stretch of arteries already isolated from mice is to examine the results of the force-length curves and find the point where the force is the same for different pressures (in our case pressures of 60, 100, and 140 mmHg). The axial stretch corresponding to this common axial force represents the *in vivo* axial stretch, where the axial force remains relatively constant as the pressure is cycled. We

compared the 60, 100, and 140 mmHg force-length curves for each artery to each other to find the intersection points between each two curves (which we calculated by interpolating between the two closest axial stretch points) and the three intersection points were averaged to yield an estimate for that vessels' *in vivo* axial stretch $\lambda_{z\ in\ vivo}$, and the corresponding axial load $f_{in\ vivo}$. We also performed ANOVA on those $\lambda_{z\ in\ vivo}$ values for $p < 0.05$, with means separation using Bonferroni's post-hoc test.

The outer diameters measured in response to the various agonists in the functional test were normalized to the final passive diameter and compared using ANOVA for $p < 0.05$, with means separation using Bonferroni's post-hoc test. Comparisons were made between mouse genotypes for all data analyses.

Results

Functional Response

Arteries from all three genotypes retained smooth muscle and endothelial function, (Table 1). The vessels were partially constricted at the beginning of the test, with diameters that were 88% of the final passive diameter for the wild-type group, 86% for the *mdx* and 85% for the *sgcd-/-*; therefore, the level of vascular basal tone developed was between 12-15%. After dosing with PE, the wild-type arteries constricted further to 67% of their final resting diameter, the *mdx* arteries constricted to 66%, and the *sgcd-/-* constricted significantly more than either the *mdx* or wild-type arteries, to 62% of their final passive diameter. For the remainder of the functional test, the three groups of vessels did not display any significant differences in response to the agonists. All groups had a similar vasodilatory response to CCh, with the wild-type dilating to 84%, and the *mdx* and *sgcd-/-* dilating to 82% of their final passive diameter. In response to SNP, the wild-type arteries dilated to 97% of their final diameter, whereas the *mdx*

and *sgcd-/-* dilated to 95%. When the media was changed to the calcium-free salt solution with EGTA, the arteries dilated slightly to reach their final passive diameter. Figure 2 shows the representative functional behavior of one vessel from each mouse type.

Mechanical Response

The general mechanical response of these three groups of mouse carotid arteries to biaxial testing was similar to that reported for other mouse carotids tested in our lab (FVB/N)[15] and elsewhere (C57-B110)[28]. In the pressure diameter tests, the arteries distended substantially in response to increasing pressure, but began stiffening at higher pressures. The sudden stiffening was more apparent in the passive testing, as the active *P-d* curves displayed a more linear response due to the influence of smooth muscle cell contraction. Vessels of the three mouse groups responded similarly for pressure cycles at the low (λ_z =1.65) and mid (λ_z =1.80) axial stretches; there were no significant differences between either the *mdx* or *sgcd-/-* and wild-type outer diameters at these axial stretches. Differences between groups were accentuated at the high (λ_z =1.95) axial stretch and mid-to-high pressures (Figure 3) as the diameters were significantly smaller in the active and passive tests for both *mdx* and *sgcd-/-* compared to the wild-type. The axial forces required to maintain a constant axial stretch during the *P-d* test were similar for all three mouse groups at the low axial stretch of 1.65. At the mid stretch of 1.80, however, the *mdx* axial force values were significantly greater at the high pressures. At the high stretch of 1.95, the *mdx* axial force values were significantly greater for the whole pressure range, while the *sgcd-/-* values were greater only at high pressures. The circumferential stress-strain data showed that only *mdx* stresses were significantly different from those of the other mouse types. The *mdx* circumferential stress σ_θ values were significantly increased compared to the wild-type stresses for a small range of circumferential stresses for the low and mid axial

Table 1: Comparison of mouse and vessel properties for wild-type, *mdx*, and *sgcd-/-* mice

	ACTIVE			PASSIVE		
	Wild-type	***mdx***	***sgcd-/-***	**Wild-type**	***mdx***	***sgcd-/-***
			Animal Properties [a]			
Body Weight (g)	27.3± 1.01	29.1 ± 1.20	26.7± 1.01	--	--	--
			Vessel Properties			
***V* (mm³)** [b]	0.338 ± 0.03	0.360 ± 0.03	0.331± 0.03	--	--	--
$\lambda_{z\ in\ vivo}$ [c]	1.88 ± 0.02	1.74 ± 0.02*	1.78 ± 0.02*	1.84 ± 0.02	1.72 ± 0.02*	1.73 ± 0.02*
			Unloaded dimensions [d]			
***OD* (µm)**	392 ± 10	406 ± 11	383 ± 10	424 ± 10	432 ± 11	416 ± 10
***A* (µm)**	123 ± 6	131 ± 6	119 ± 6	148 ± 6	152 ± 6	145 ± 6
***H* (µm)**	72.7 ± 3	71.5 ± 3	72.2 ± 3	63.3 ± 3	63.6 ± 3	62.9 ± 2
			Functional response [e]			
Basal Tone	0.881 ± 0.02	0.861 ± 0.02	0.854 ± 0.02	--	--	--
Contraction to PE	0.666 ± 0.01	0.660 ± 0.01	0.617 ± 0.01*	--	--	--
Dilation to CCh	0.844 ± 0.02	0.820 ± 0.02	0.821 ± 0.02	--	--	--
Dilation to SNP	0.974 ± 0.01	0.953 ± 0.01	0.947 ± 0.01	--	--	--

All data are represented as mean ± s.e.m., and a * indicates statistical significance when either the mdx or sgcd-/- value is compared to the wild-type ($p < 0.05$ with Bonferonni's post-hoc test for means separation).

[a] These values are the average body weights of mice tested for each mouse type. No significant differences were found.

[b] These values are the calculated mean volumes of the vessels tested for each mouse type.

[c] This set of data is the mean *in vivo* axial stretches ($\lambda_{z\ in\ vivo}$) inferred from axial force-length active and passive testing for each mouse type.

[d] These values are the mean unloaded outer diameters (*OD*), inner radii (*A*), and wall thicknesses (*H*) for each mouse type measured at the start of the active and passive mechanical tests.

[e] This set of data is from the function test results and shows outer diameters in response to agonists normalized to the final, most dilated diameter of the vessel in response to calcium-free HBSS with EGTA and SNP. The first row of values was measured after equilibration to testing conditions (Basal tone), the second after contraction to phenylephrine (PE), the third after dilation to carbamylcholine chloride (CCh), and the fourth after dilation to sodium nitroprusside (SNP).

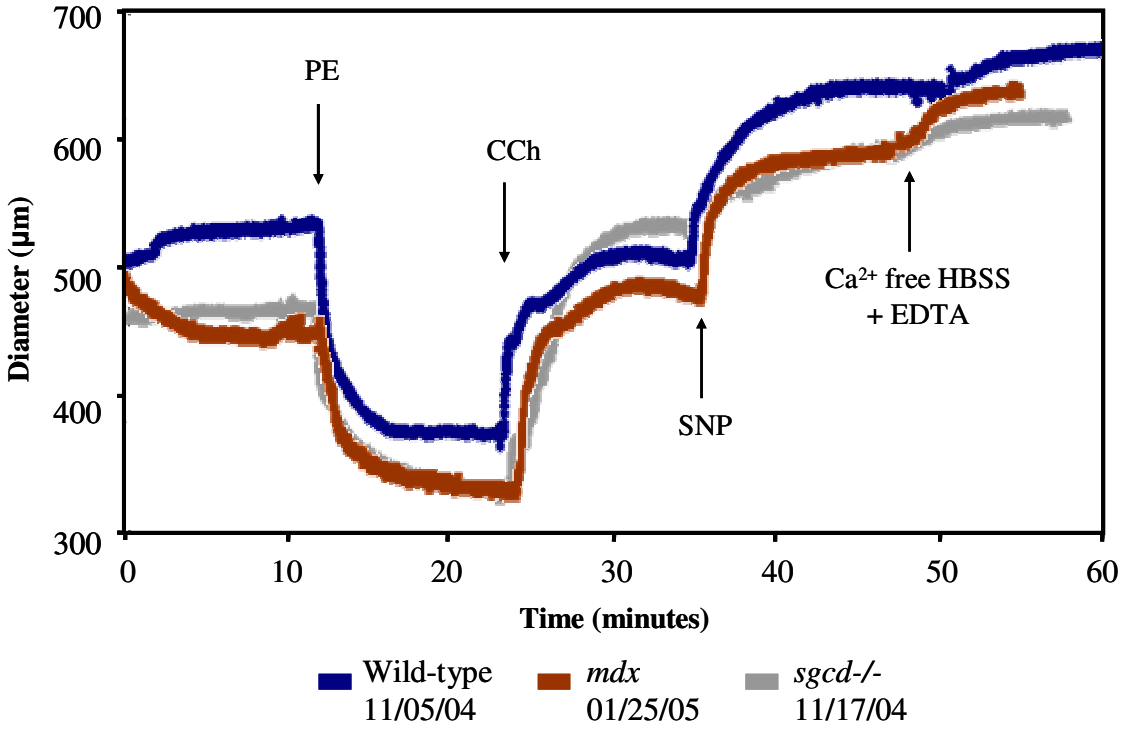

Figure 2: Representative functional response of vessels of all three mouse types. The change in outer diameter in response to agonists of a wild-type vessel tested 11/05/04, an *mdx* vessel tested 1/25/05, and a *sgcd-/-* vessel tested 11/17/05 are graphed over time. Phenylephrine (PE) was used to test for smooth muscle contraction, carbamylcholine chloride (CCh) was used to test for endothelial-dependent smooth muscle dilation, and sodium nitroprusside (SNP) was used to test for endothelial-independent smooth muscle dilation. Calcium-free salt solution (HBSS) with a calcium chelator (EGTA) was used to relax the smooth muscle cells completely.

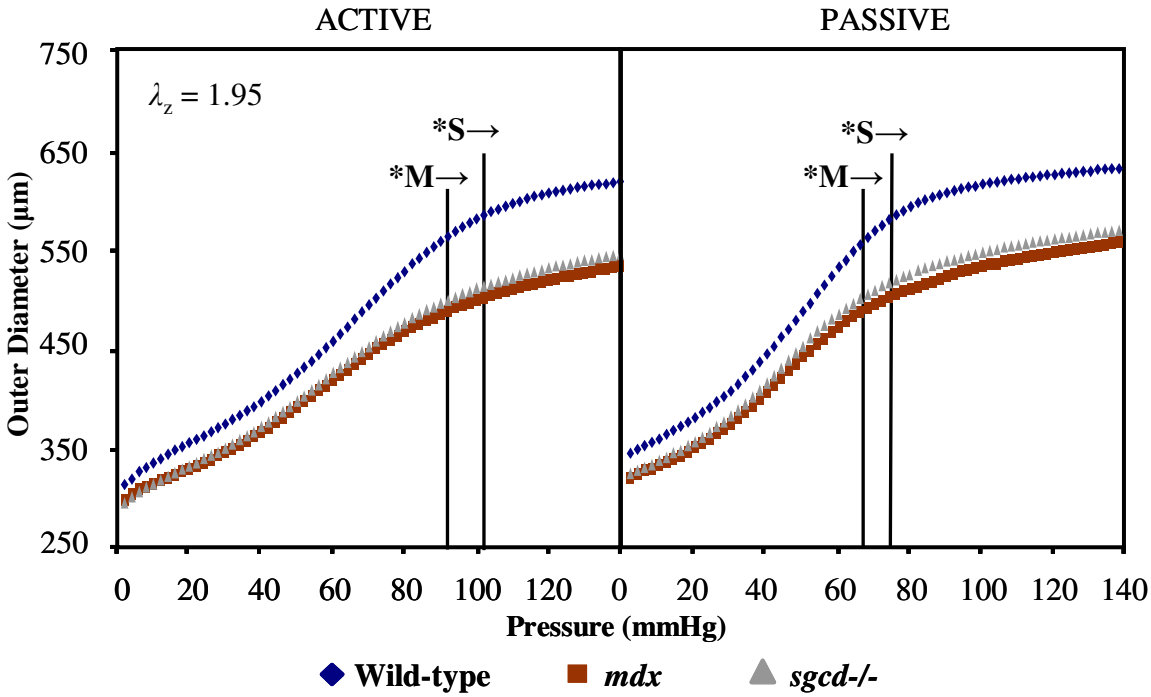

Figure 3: Active (basal tone) and passive (Ca^{2+} free) *P-d* curves at the high (λ_z =1.95) axial stretch setpoint. Note that the diameters for the *mdx* and *sgcd-/-* tend to be smaller. The *mdx* values become significantly different ($p < 0.05$) from the wild-type over the pressure range P = 92 – 140 in the active state and at P = 66 – 140 in the passive state (indicated by the ***M→**). The *sgcd-/-* values are significantly different for the pressure range P = 102 – 140 in the active state and P = 74 – 140 in the passive state (indicated by the ***S→**).

stretches, and over a broader range at the high axial stretch. Figure 4 shows the circumferential stress-strain behavior at the high axial stretch, in which there is also a range of circumferential stretches in both the active and passive states at which the *mdx* circumferential stress was significantly greater than the *sgcd-/-* circumferential stress.

One interesting finding was that the axial force response at the high axial stretch of 1.95 for the wild-type was fairly constant; in contrast, the axial force for *mdx* and *sgcd-/-* vessels increased greatly. At the mid axial stretch, the *mdx* and *sgcd-/-* axial force responses were constant, whereas the wild-type axial force decreased at the mid to high pressures. When we compared all the axial force responses during pressurization for the three mouse groups at the three axial stretches, as in Figure 5, it seemed that the wild-type force response at the high axial stretch of 1.95 was similar to the *mdx* and *sgcd-/-* force responses at the mid axial stretch of 1.80. Because the axial force remains constant over a range of pressures when the axial stretch is near the *in vivo* value,[24] whereas the axial force increases at axial stretches greater than the *in vivo* and decreases at axial stretches less than the *in vivo* axial stretch, we can infer that the *in vivo* axial stretch of the carotid artery for the wild-type is greater ($\lambda_z \approx 1.95$) than that for the *mdx* and *sgcd-/-* mouse groups ($\lambda_z \approx 1.80$).

Results for the axial force-length test showed significant differences between the mouse groups occurring predominately at the high pressure of 140 mmHg and high axial stretches. The axial force corresponding to axial stretches for the *mdx* and *sgcd-/-* vessels were not significantly greater than the wild-type at the low pressure of 60 mmHg, except that the *mdx* value at very high axial stretches was significantly greater than that for the wild-type in the active and passive tests. At the mid pressure of 100 mmHg, the *mdx* and *sgcd-/-* axial forces were significantly higher than those for the wild-type for a range of high axial stretches in the active and passive

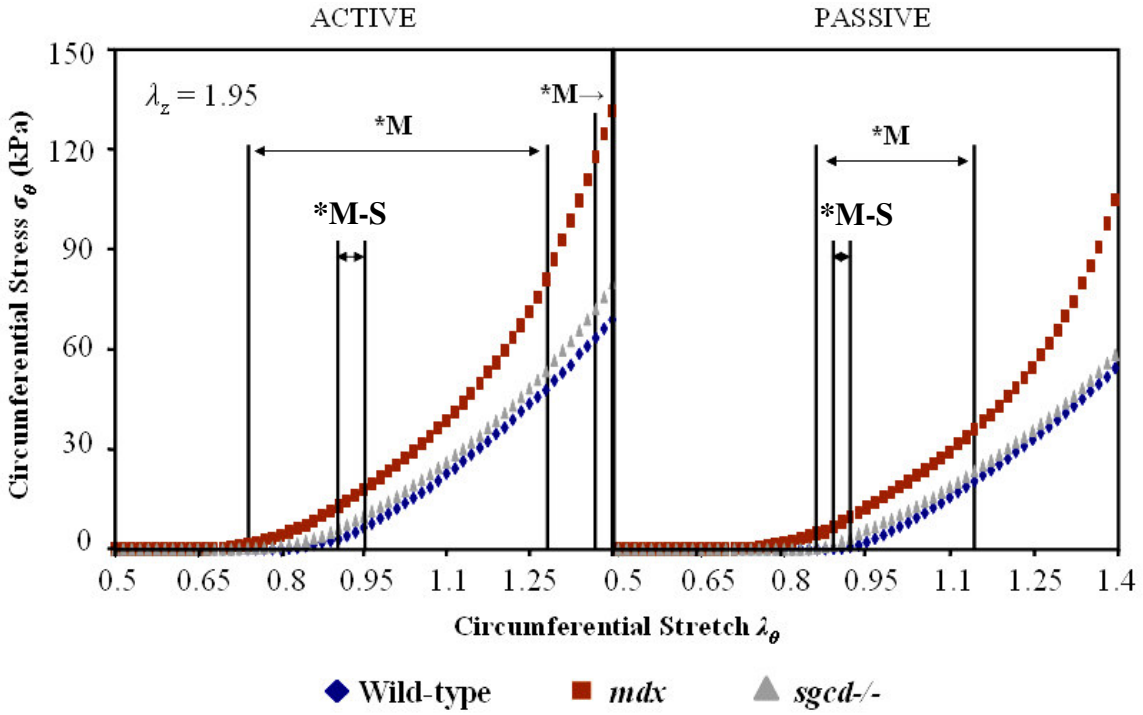

Figure 4: Active (basal tone) and passive (Ca^{2+} free) circumferential stress-stretch curves at the high (λ_z = 1.95) axial stretch setpoint. There were two ranges of circumferential stretch values in the active state (λ_θ = 0.740 – 1.280, 1.370 – 1.400) and one range in the passive state (λ_θ = 0.860 – 1.145), indicated by ***M,** for which the *mdx* circumferential stresses were significantly greater ($p < 0.05$) than the wild-type values. There is also a range of in the active (0.905 – 0.950) and passive (0.890 – 0.920) state for which the *mdx* stresses were significantly greater than the sgcd-/- stresses, indicated by ***M-S**. Although there are visible trends in the data, the variance of the stresses at the high stretch values prevented statistical differences from being reported over a wider range of values.

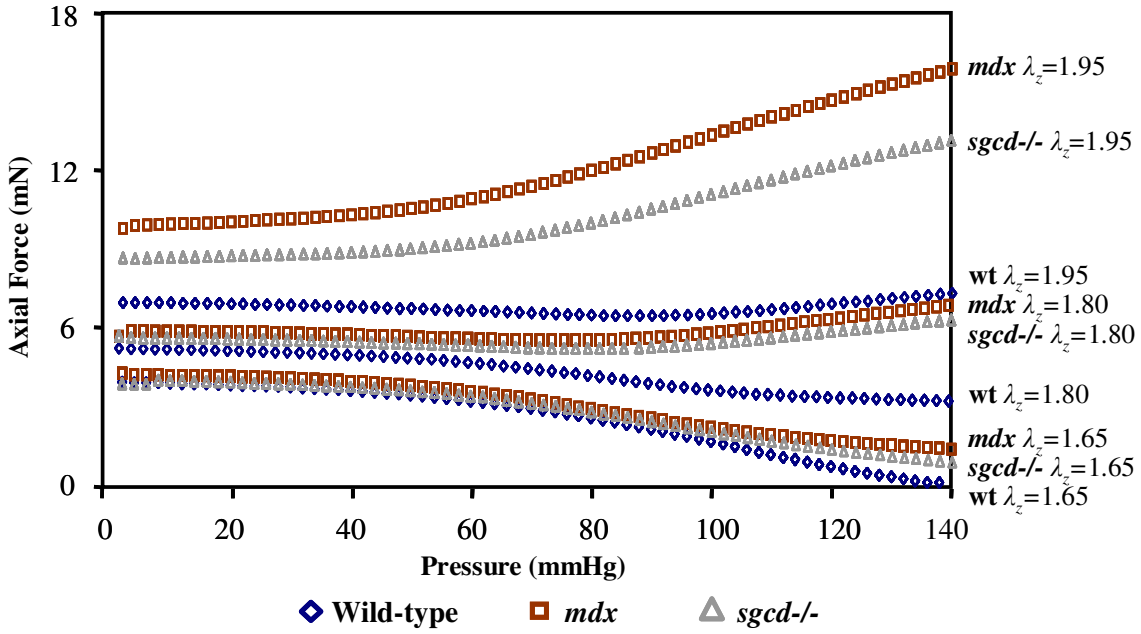

Figure 5: Active axial force response during *P-d* test for all mouse groups at all axial stretch setpoints. Mouse type (wt = wild-type) and axial stretch are indicated on the right axis where the curve ends. Note the similarity between the wild-type curve at the high axial stretch (λ_z =1.95) and the *mdx* and *sgcd-/-* curves at the mid axial stretch (λ_z =1.8).

states. At the high pressure of 140mmHg, the *mdx* and *sgcd-/-* axial force values were significantly higher than the wild-type at mid-range axial stretches in the active and passive states.

The axial stress-stretch data were similar to the axial force-length data despite subtle differences. There were few significant differences between groups in the axial stress-stretch data at the low pressure for the active test. At the mid pressure, there were significant differences between both *sgcd-/-* and *mdx* values as compared to the wild-type, with a larger range of significant differences in the passive than the active state. At the high pressure, there was a broad

range of axial stretches for both *mdx* and *sgcd-/-* at which the axial stresses were significantly higher than the wild-type (Figure 6). These differences were again more pronounced in the passive test. Table 2 shows the ranges at which results for the various mechanical tests were statistically different between mouse types.

We estimated the *in vivo* axial stretch ($\lambda_{z\ in\ vivo}$) by calculating the intersection point between the three force-length curves for each vessel, (measured at the low, mid, and high *P* set-points as shown in Figure 7) and found that the wild-type vessels had a significantly higher *in vivo* axial stretch as compared to *mdx* and *sgcd-/-*. The axial load required to maintain the *in vivo* axial stretch was significantly lower for *mdx* and *sgcd-/-* vessels than for the wild-type. The average passive and active *in vivo* axial stretches and corresponding axial loads for the three types are shown in Figure 8. The values for the passive and active *in vivo* axial stretches $\lambda_{z\ in\ vivo}$ were also included in Table 1 with the average unloaded dimensions of the vessels for each mouse type.

Normalization to* in vivo *Axial Stretch

With the observation concerning the axial force-pressure data, that is, that the wild-type curve for the high axial stretch looked similar to the *mdx* and *sgcd-/-* curves for the mid axial stretch, additional comparisons were warranted. For the *P-d* test, we calculated the stretch ratio $\Lambda = \lambda_z / \lambda_{z\ in\ vivo}$ for the high ($\lambda_z = 1.95$), mid ($\lambda_z = 1.80$), and low ($\lambda_z = 1.65$) axial stretches used in testing and for the estimated *in vivo* axial stretch of each mouse type. We found that for the active and passive *P-d* tests, the wild-type vessels experienced a small Λ at the high axial stretch (~1.03 for the active and ~1.06 for the passive) which was very close to that experienced by the *mdx* (~1.03 active, ~1.05 passive) and *sgcd-/-* (~1.01 active, ~1.04 passive) vessels at the mid axial stretch. That is, the *mdx* and *sgcd-/-* vessels experienced a small amount of axial stretch, relative to the axial stretch they feel *in vivo*, when *P-d* tests were conducted at the mid axial

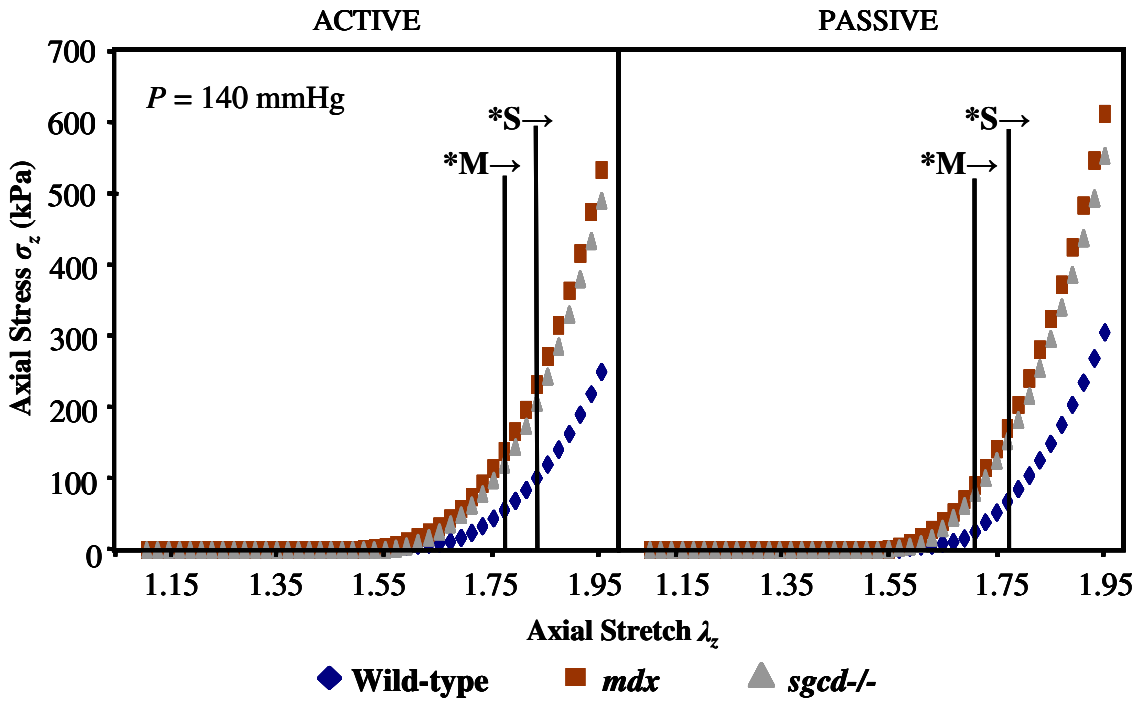

Figure 6: Active (basal tone) and passive (Ca^{2+} free) axial stress-stretch curves at the high (P = 140 mmHg) pressure setpoint. The axial stresses for the *mdx* and *sgcd-/-* tend to be greater than the wild-type over wide ranges in both the active and passive states. The *mdx* values become significantly different ($p < 0.05$) from the wild-type over the axial extension range λ_z = 1.77– 1.95 in the active state and at λ_z = 1.83 – 1.95 in the passive state (indicated by the ***M→**). The *sgcd-/-* values are significantly different for the pressure range λ_z = 1.83 – 1.95 in the active state and λ_z = 1.77 – 1.95 in the passive state (indicated by the ***S→**).

Table 2: Summary of significant differences for mechanical tests

	Range of values on which ANOVA was performed	Range of values over which statistical significance ($p < 0.05$) was observed					
		ACTIVE			PASSIVE		
		mdx versus wt	*sgcd -/-* versus wt	*mdx* versus *sgcd -/-*	*mdx* versus wt	*sgcd -/-* versus wt	*mdx* versus *sgcd -/-*
Diameter-pressure [a]	over P	*Outer diameter*					
Testing $\lambda_z = 1.65$	2–140	NS	NS	NS	NS	NS	NS
Testing $\lambda_z = 1.80$	2–140	NS	NS	NS	NS	NS	NS
Testing $\lambda_z = 1.95$	2–140	92–140	102–140	NS	66–140	74–140	NS
Force-pressure [b]	over P	*Axial force*					
Testing $\lambda_z = 1.65$	2–140	NS	NS	NS	128–140	NS	NS
Testing $\lambda_z = 1.80$	2–140	120–140	NS	NS	86–140	110–140	NS
Testing $\lambda_z = 1.95$	2–140	2–140	82–140	NS	50–140	54–140	NS
Circumferential stress-stretch [c]	over λ_θ	*Circumferential stress*					
Testing $\lambda_z = 1.65$	0.500–1.400	NS	NS	NS	1.010–1.115	NS	NS
Testing $\lambda_z = 1.80$	0.500–1.400	0.935–1.025	NS	NS	0.980–1.040	NS	NS
Testing $\lambda_z = 1.95$	0.500–1.400	0.740–1.280, 1.370–1.400	NS	0.905–0.950	0.860–1.145	NS	0.890–0.920
Axial force-length [d]	over λ_z	*Axial force*					
Testing P = 60mmHg	1.11–1.95	1.95	NS	NS	1.91–1.95	NS	NS
Testing P = 100mmHg	1.11–1.95	1.85–1.95	1.91–1.95	NS	1.77–1.95	1.83–1.95	NS
Testing P = 140mmHg	1.11–1.95	1.75–1.95	1.81–1.95	NS	1.73–1.95	1.77–1.95	NS
Axial stress-stretch [e]	over λ_z	*Axial stress*					
Testing P = 60mmHg	1.11–1.95	NS	NS	NS	1.95	NS	NS
Testing P = 100mmHg	1.11–1.95	1.89–1.95	1.93–1.95	NS	1.77–1.95	1.83–1.95	NS
Testing P = 140mmHg	1.11–1.95	1.77–1.95	1.83–1.95	NS	1.71–1.95	1.77–1.95	NS

Data shown are ranges of statistical significance ($p < 0.05$ with Bonferonni's post-hoc test for means separation) for various mechanical tests in the active and passive states for the different comparisons between mouse types, that is, for *mdx* versus wild-type (wt), *sgcd-/-* versus wild-type (wt), and *mdx* versus *sgcd-/-*. "NS" indicates no significant differences for that test for the different comparisons between mouse types.

[a] This set of data is for the pressure-diameter results and shows the pressure range over which outer diameters were significantly different.

[b] This set of data is for the pressure-force results and shows the pressure range over which axial forces were significantly different.

[c] This set of data is for the circumferential stretch-stress results and shows the circumferential stretch range over which circumferential stresses were significantly different.

[d] This set of data is for the axial force-length results and shows the axial stretch range over which axial forces were significantly different.

[e] This set of data is for the axial stretch-stress results and shows the axial stretch range over which axial stresses were significantly different.

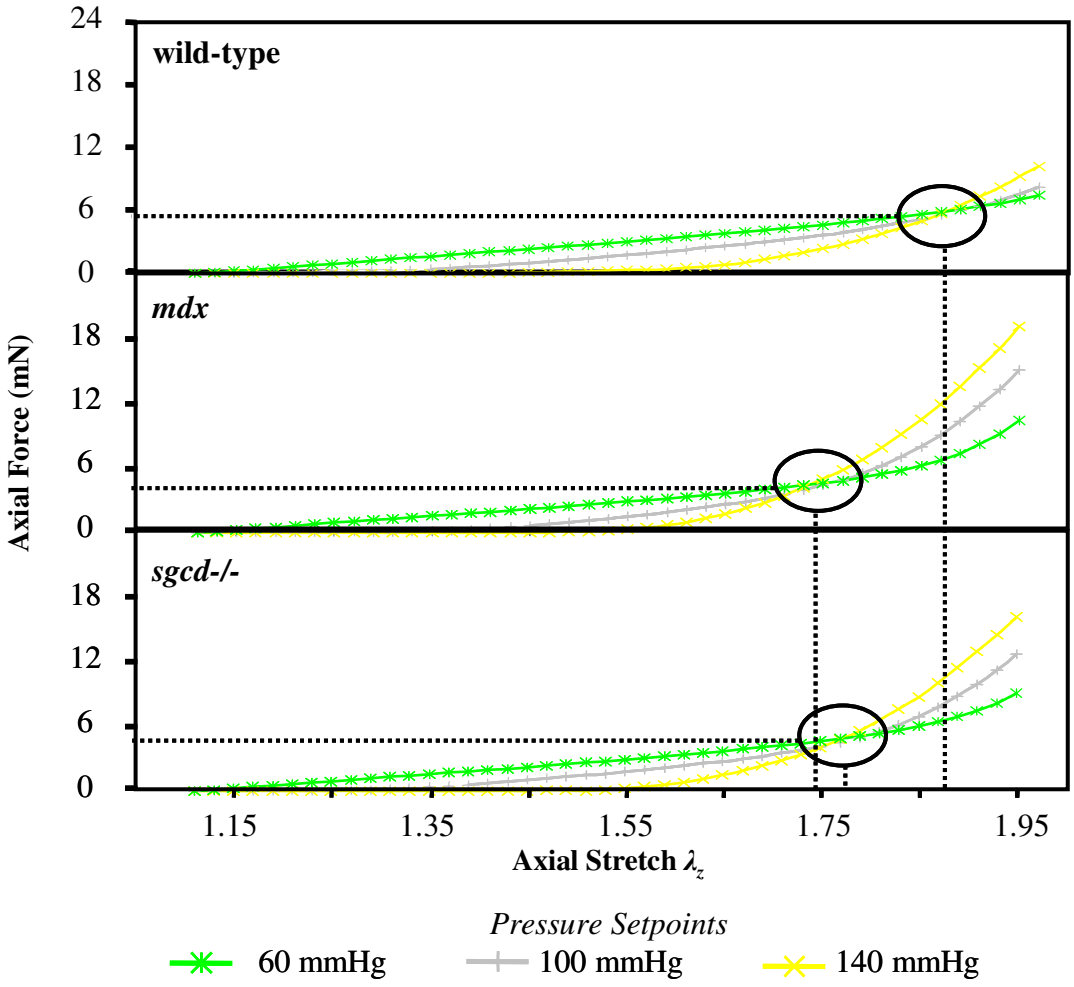

Figure 7: Estimation of the *in vivo* axial stretch ($\lambda_{z\ in\ vivo}$). We calculated the intersection point between the three force-length curves for each vessel, (measured at the low, mid, and high *P* set- points) to estimate the in vivo axial stretch, the axial stretch at which the axial load remains constant over pressure, and the corresponding in vivo axial load sustained at that axial stretch for each mouse type.

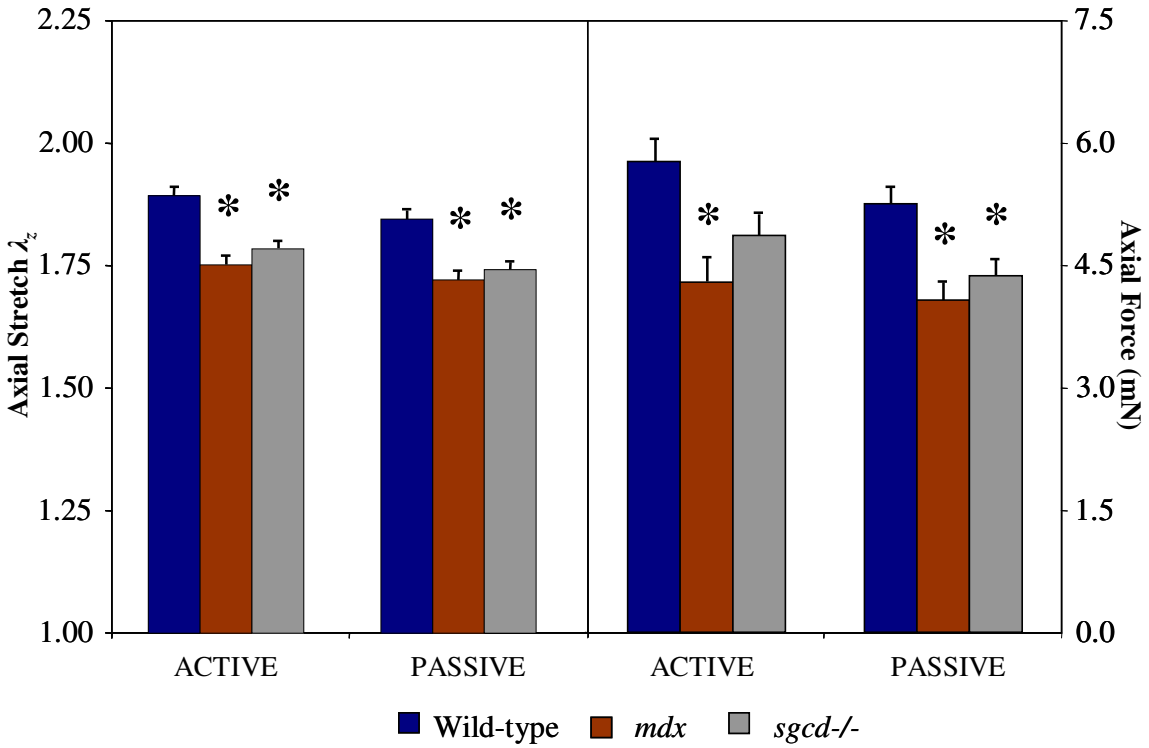

Figure 8: Average axial stretch λ_z and axial force values (with standard errors) at which the average axial *f-ℓ* curves for each mouse type, measured at three different pressure setpoints, intersect in the active (basal tone) and passive (Ca^{2+} free) states. This intersection point between *f-ℓ* curves represents the *in vivo* axial stretch, at which the axial load remains constant for any pressure. A * indicates significant differences of the *mdx* and *sgcd-/-* values from the wild-type ($p < 0.05$) with Bonferonni's test for means separation.

stretch. The wild-type vessels experienced a similar small amount of stretch beyond their *in vivo* axial stretch at the high axial stretch used for *P-d* tests. We then compared the wild-type outer diameters at the high axial stretch of 1.95 to the *mdx* and *sgcd-/-* values at the mid axial stretch of 1.8 and found that no significant differences ($p < 0.05$) were present in either the active or passive tests (Figure 9). There were also no significant differences between the circumferential stress-stretch data measured at the high axial stretch for the wild-type and the mid axial stretch for the *mdx* and *sgcd-/-* values (Figure 10).

Finally, for the *f-ℓ* test, we again calculated the stretch ratio Λ by normalizing all measured axial stretches λ_z to the *in vivo* axial stretches ($\lambda_{z\ in\ vivo}$) estimated for each mouse type. Then we compared the axial loads and stresses to common values of the stretch ratio Λ. We found that this way of comparing the data reduced the number of significant differences between the wild-type and the *mdx* and *sgcd-/-* vessels. For tests in active or passive states at the high pressure of 140 mmHg, there were no significant differences between mouse types in the axial load or axial stress once we took the *in vivo* axial stretch into account (Figure 11). At the pressures of 60 and 100 mmHg, there were also no significant differences between the *sgcd-/-* and wild-type for axial load or axial stress values. Indeed, there were only significant differences between the *mdx* and wild-type over a small range of stretches at the mid pressure and over a larger range of stretches at the low pressure for both the axial load and axial stress.

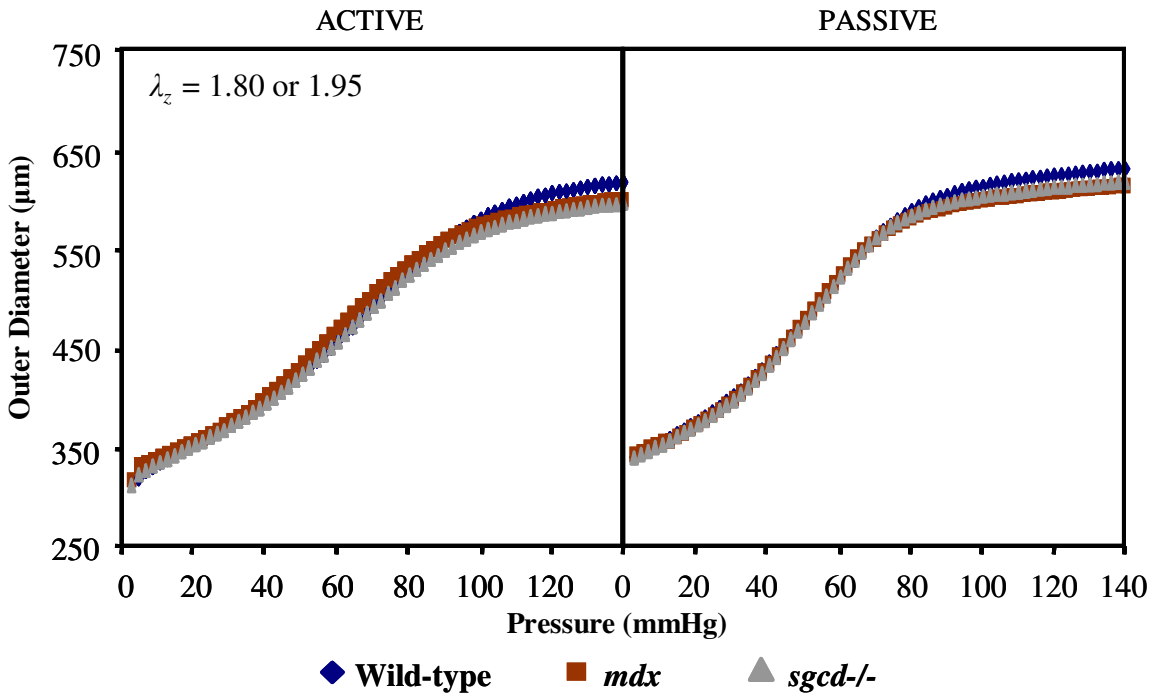

Figure 9: Active (basal tone) and passive (Ca^{2+} free) *P-d* curves at the high (λ_z = 1.95) axial stretch setpoint for the wild-type and at the mid (λ_z = 1.80) axial stretch setpoint for the *mdx* and *sgcd-/-* arteries. Comparing the results from these two different axial stretch setpoints allows us to see the change in diameter over pressurization for all three groups of vessels when stretched to ~1.05 of their *in vivo* axial stretch. The diameter values for the *mdx* and *sgcd-/-* are no longer significantly different from the wild-type in either the active or passive state ($p < 0.05$) when the estimated *in vivo* axial stretch is taken into account for each mouse type.

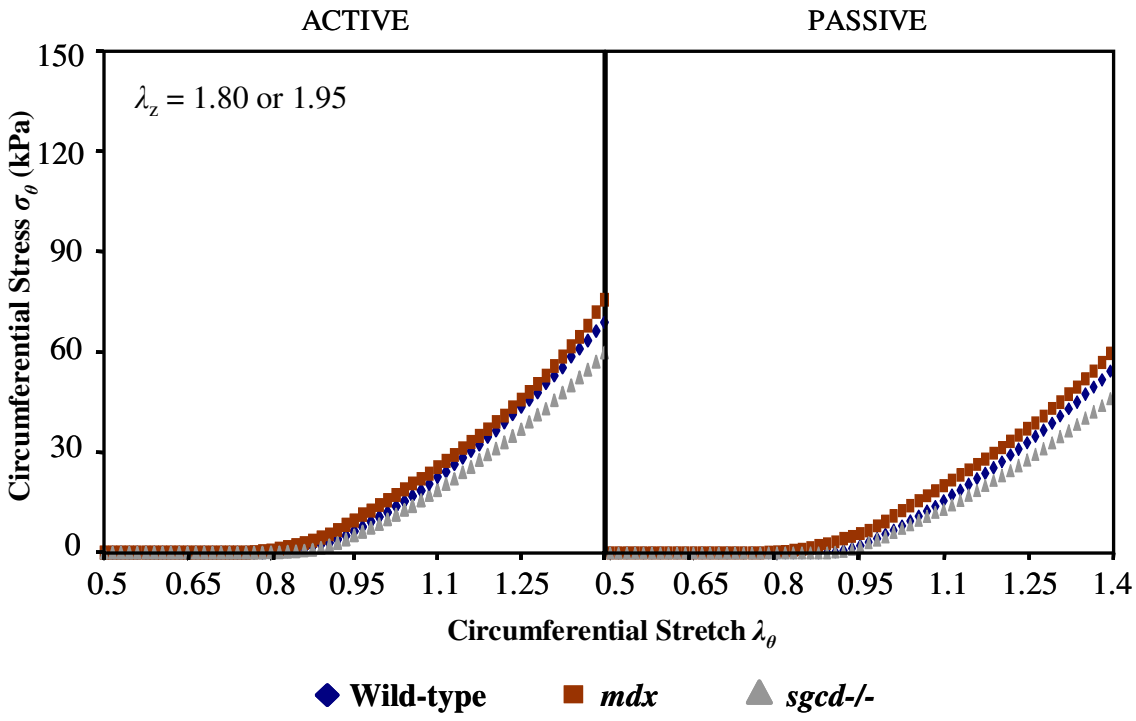

Figure 10: Active (basal tone) and passive (Ca^{2+} free) circumferential stress-stretch curves at the high (λ_z = 1.95) axial stretch setpoint for the wild-type and at the mid (λ_z = 1.80) axial stretch setpoint for the *mdx* and *sgcd-/-*arteries. Comparing the results from these two different axial stretch setpoints allows us to compare the three groups of vessels when stretched to ~1.05 of their *in vivo* axial stretch. Note that when the axial stretch is normalized to the estimated *in vivo* axial stretch for each mouse type, the circumferential stresses for the *mdx* and *sgcd-/-* are no longer significantly different from the wild-type in either the active and passive state ($p < 0.05$).

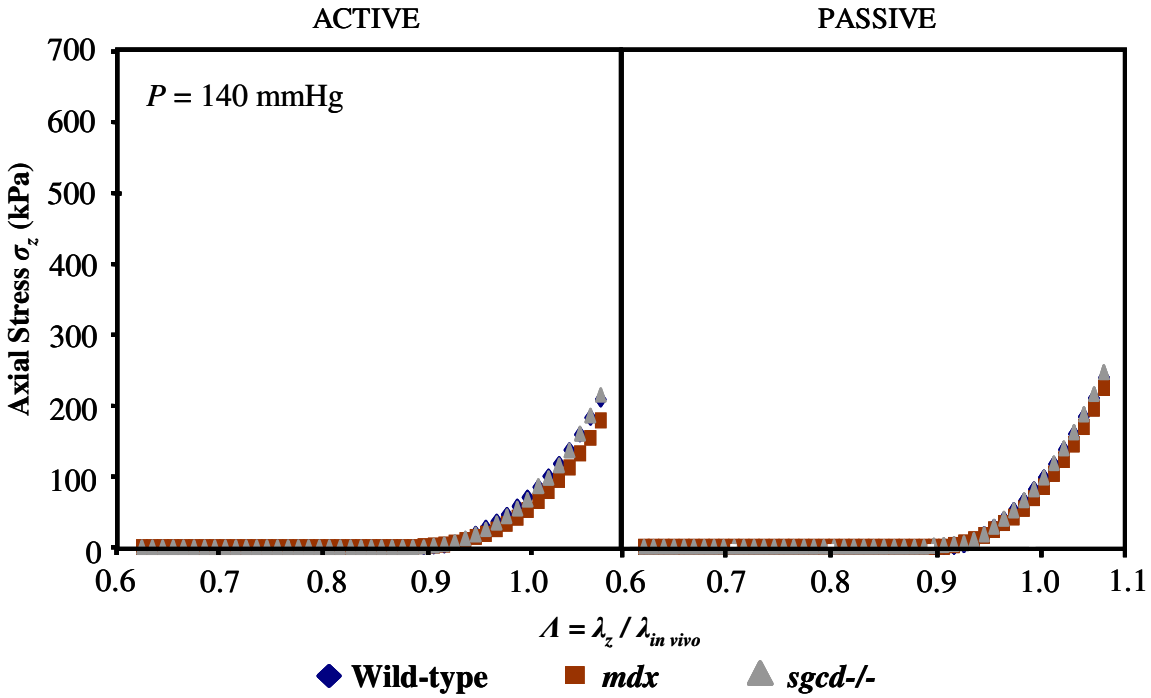

Figure 11: Active (basal tone) and passive (Ca^{2+} free) axial stress-stretch curves, with the axial stretch normalized to the *in vivo* axial stretch, at the high (P = 140mmHg) pressure setpoint. Note that when the axial stretch is normalized to the estimated *in vivo* axial stretch for each mouse type, the axial stresses for the *mdx* and *sgcd-/-* are no longer significantly different from the wild-type in either the active and passive state ($p < 0.05$)

Discussion

We found biomechanical differences between large arteries of *mdx* mice lacking dystrophin (as occurs in the human disease Duchenne's muscular dystrophy) and *sgcd-/-* mice lacking sarcoglycan-delta (as in human limb-girdle muscular dystrophy) when compared to wild-type controls. Specifically, *mdx* and *sgcd-/-* carotid arteries did not distend as much as wild-type arteries, and *mdx* arteries exhibited increased circumferential mean stresses in pressure-diameter testing. Also, *mdx* and *sgcd-/-* arteries exhibited higher axial forces and mean axial stresses, as compared to wild-type arteries, during axial force-length testing. The pressure-diameter testing also showed that the axial force required to maintain a constant stretch was greater for *mdx* and *sgcd-/-* arteries than for wild-type arteries at mid and high axial stretches. These differences were present in both active and passive SMC states, although the functional response and unloaded dimensions of *mdx*, *sgcd-/-*, and wild-type arteries were similar.

One way to explain the mechanical behaviors of the *mdx* and *sgcd-/-* arteries involves a shift in the phenotype of the vascular SMCs in these arteries from the differentiated, contractile phenotype to the dedifferentiated, synthetic phenotype. The phenotype of vascular SMCs is intimately associated with the extracellular matrix (e.g., laminin, fibronectin, elastin, collagen, and glycosaminoglycans) that surrounds the cells.[24] Linkages between the vascular SMCs and the extracellular matrix are made by transmembrane proteins, namely integrins, but also through syndecans, cell adhesion molecules (CAMs), and the DGC.[34] α-Dystroglycan is the specific extracellular component of the DGC that connects muscle cells to the extracellular matrix by binding to laminin. Laminin binding to vascular SMCs signals the cells to take on the contractile phenotype, as characterized by expression of α-smooth muscle actin and the presence of structural myofilaments.[48,21] Fibronectin binding, on the other hand, seems to be involved in dedifferentiation of vascular SMCs to the synthetic phenotype and is associated with early

development and injury to the vascular system.[48] A normal part of development for muscle cells is a switch in phenotype from synthetic and proliferative to contractile that begins to occur just prior to birth (>80% of SMCs are actively replicating) and continues through early postnatal life (~40% SMC replication) until the majority of SMCs are differentiated and contractile in adulthood (<0.06% SMC replication).[26, 46] It may be that in development of arteries lacking a functional DGC, the link between vascular SMCs and laminin that stimulates differentiation is made incompletely or is delayed, while fibronectin linkages continue to stimulate synthetic activity. Changes in vascular SMC linkages to the ECM could be effected by integrins, which are heterodimeric, transmembrane proteins with paired α and β subunits and ligand-binding specificity. Abnormal expression of integrins occurs when the DGC is absent. Specifically, $\alpha_7\beta_1$ is upregulated in muscle of *mdx* and *sgcd-/-* mice[2] as well as in DMD patients.[22] $\alpha_7\beta_1$ links the cytoskeleton of muscle cells to laminin, and may partly compensate for the lack of laminin binding in the absence of an intact DGC. Yet, $\alpha_5\beta_1$ is also increased in *mdx* and *sgcd-/-* mice. This integrin is a major fibronectin linkage for myofibers and was found in conjunction with fibrosis and regenerating skeletal muscle fibers.[2] The increase of both $\alpha_7\beta_1$ and $\alpha_5\beta_1$ integrins may represent two groups of vascular SMCs, some that form a laminin connection via integrins in the absence of the DGC to establish the contractile phenotype and others that instead link to fibronectin and maintain a synthetic phenotype. It has been noted that heterogeneity of SMC phenotype is characteristic in normal vascular tissue, and that this cellular diversity equips the blood vessel to maintain vascular homeostasis in normal or pathologic conditions.[46] But, perhaps in the *mdx* and *sgcd-/-* arteries the fine balance of contractile and synthetic SMCs is perturbed when binding to laminin via the DGC is compromised. Through increased binding to fibronectin, more vascular SMCs may remain in the synthetic phenotype and secrete ECM components such as collagen I and III. In fact, the abnormal deposition by muscle cells of collagen to the extra-

cellular matrix, which results in fibrosis, is a hallmark of muscular dystrophy.[3] An overabundance of these structural proteins in the arteries of *mdx* and *sgcd-/-* mice could explain the altered mechanical properties that we observed. It may be possible to measure a collagen mass fraction from frozen sections taken from wild-type, *mdx*, and *sgcd-/-* carotid arteries to quantify any changes in the amount of collagen present in the ECM.

A secondary explanation for the upregulation of $\alpha_5\beta_1$ in *mdx* and *sgcd-/-* mice is that its heightened levels represent muscle regeneration, as this integrin is present in developing myofibers. Muscle degeneration and regeneration is characteristic of muscular dystrophy in humans and animals, and occurs in skeletal muscle of *mdx* mice.[40] Indeed, *mdx* mice have the capacity to regenerate sufficient amounts of functional muscle and display a much milder disease phenotype, characterized by a normal life-span with no overt muscle weakness, than that of DMD.[6] Perhaps the vascular SMCs that are not able to compensate for the loss of the DGC linkage suffer necrosis, but proliferation of the healthy SMCs replaces the damaged and dying muscle cells. The developing vascular SMCs may thus be able to forge a link to laminin through $\alpha_7\beta_1$ or by upregulating utrophin, a protein with binding domains that are remarkably similar to dystrophin. If utrophin expression is high enough, it can take the place of dystrophin in associating with the DGC,[31] and utrophin expression is high in regenerating *mdx* muscle fibers.[27] Utrophin replacement of dystrophin in regenerating fibers of *mdx* mice may be partially responsible for the mild disease phenotype, as supported by the fact that dystrophin/utrophin deficient mice display an early onset of muscular dystrophy and die prematurely, similar to patients with DMD.[12] Although utrophin activity could change the mechanical properties of the arteries in *mdx* mice by replacing dystrophin, it should not change the state of the DGC in *sgcd-/-* mice that possess functional dystrophin. Yet, our results showed remarkably similar mechanical behavior between arteries of mice missing dystrophin and the arteries of mice lacking

sarcoglycan-delta but possessing dystrophin, suggesting that the absence of an intact and functional DGC in both mouse types is responsible for the changes in mechanical behavior. An assay to determine the expression of proteins such as utrophin and the integrins $\alpha_5\beta_1$ and $\alpha_7\beta_1$ integrins in the *mdx* and *sgcd-/-* vascular smooth muscle is needed before any conclusions can be made.

This leads us to another explanation of our results involving the significant increases in axial force exerted during *P-d* testing by the *sgcd-/-* and *mdx* arteries. We investigated this result further by calculating an estimate of the *in vivo* axial stretch ratio by finding the intersection of the axial *f-ℓ* curves taken at different pressure setpoints (expecting that at the *in vivo* axial stretch, the axial force needed to maintain the stretch will remain fairly constant over a range of pressures). The estimates for the *in vivo* axial stretch suggested that *mdx* and *sgcd-/-* carotid arteries had a reduced *in vivo* axial stretch ratio compared to wild-type arteries. Although we did not measure the axial stretch of the mouse arteries *in vivo* and *ex vivo* to confirm the difference in the *in vivo* axial stretch ratio between the knockouts and the wild-type, our mechanical data suggested strongly that there was a true difference between the wild-type and knockout mice. We normalized our raw data using calculated estimates of the *in vivo* axial stretch ratio for all three mouse types, and found that this drastically reduced the significant differences we had seen. In particular, there were no longer differences between *mdx* or *sgcd-/-* and wild-type outer diameter values and circumferential stresses measured in the *P-d* test or axial forces and stresses measured in the *f-ℓ* test. The only significant differences that persisted were decreased axial forces during pressurization in active and passive *P-d* tests for the *mdx* arteries compared to wild-type. It seems that *mdx* and *sgcd-/-* arteries have somehow decreased their *in vivo* axial stretch to a level at which their response to mechanical stimuli is nearly identical to the arteries of normal, wild-type mice.

These results reaffirm that axial stress is an important factor driving vascular remodeling of large arteries, although it has been little studied in comparison to hoop stress and shear stress, two other factors that also play a role in remodeling. Axial, or longitudinal, forces are imposed on arteries by connections to peri-arterial tissues and result in axial stretches, which are displayed in the retraction blood vessels undergo when isolated from the rest of the vascular system. Studies conducted on vascular remodeling caused by changes in axial stretch (and thereby axial force) have shown that increases in axial tension can be normalized rapidly by smooth muscle cell growth and remodeling without the loss of vascular function. Mouse carotid arteries cultured at axial stretches greater or less than their *in vivo* axial stretch exhibited changes in their force-pressure character, probably by reorientation of SMCs, to approximate the *in vivo* character in only two days.[16] Axial stretch increases of 50% of rabbit carotid arteries *in vivo* were normalized in one week as, through SMC and extracellular matrix (ECM) proliferation, the vessel "grew to a new length".[25,17] Porcine carotid arteries stretched incrementally to ~50% of their physiological axial length over 9 days in culture were found, upon removal from the system, to be lengthened 20% as compared to their initial unloaded configuration.[7] The increased axial stretches imposed on the vessels in these studies had the effect of increasing the axial force f and thereby the axial stress σ_z; these increases were sensed by vascular SMCs and normalized by growth and rearrangement of the cells and the surrounding ECM.

Why do *mdx* and *sgcd-/-* mouse carotid arteries adopt a decreased *in vivo* axial stretch, at which the axial load is maintained constant over a range of pressures, as compared to the wild-type? It seems that the *mdx* and *sgcd-/-* arteries have adapted to a decreased axial stretch at which they were able to respond to imposed mechanical stresses the way wild-type arteries did at an increased *in vivo* axial stretch. We can postulate that this decreased axial stretch was established in *mdx* and *sgcd-/-* mice *in vivo* through development to compensate for the

important DGC transmembrane link to the ECM that is absent in these SMCs. It may be that for the *mdx* and *sgcd-/-* arteries, the axial tension felt by the SMCs is increased in the absence of an intact DGC, which is thought to redistribute local mechanical stresses imposed on the muscle cell membranes throughout the cell cytoskeleton and to the extracellular matrix, thus protecting the cell membrane from damage.[38] Without the link the DGC provides between the SMC cytoskeleton and the ECM, the SMCs may not be able to bear the axial stresses imposed on them and they begin to reorient, grow and/or proliferate to lengthen the vessel and thereby attenuate the axial stresses on the SMCs, as in the stretch studies mentioned earlier. Part of this lengthening process may be hypertrophy of the circumferentially oriented SMCs, which correlates well with the hypertrophy of skeletal muscle fibers that is characteristic of muscular dystrophy and occurs in young *mdx* mice.[39] At the new, decreased axial stretch to which the vascular SMCs adapt the vessel, the corresponding average axial load exerted by the vessel is decreased (Figure 8). Figure 12 demonstrates that the *mdx* and *sgcd-/-* vessels have slightly reduced the axial load they must exert to maintain their reduced *in vivo* axial stretch over a range of pressures. It seems that there has been a remodeling event, changing the state of the vascular SMCs and the ECM (as evidenced by changes in the active and passive smooth muscle state), to decrease the axial loads and stresses imposed on the system to tolerable levels in carotid arteries of *mdx* and *sgcd-/-* mice. Notably, the *mdx* and *sgcd-/-* arteries do not seem to have remodeled in response to changed circumferential or shear stresses, as the wall thicknesses and inner and outer diameters in the unloaded and loaded states were not significantly different from the wild-type. This distinguishes the remodeling we observed from that reported in hypertension, in which decreases of the *in vivo* axial stretch of aortic segments were accompanied by increases in the wall thickness and mid-wall radius.[51] It seems that the vessel growth and remodeling in the arteries of *mdx* and *sgcd-/-* mice occurred solely to reduce the axial force, and thereby the axial

stress, while maintaining the levels of the other stresses. The vessel therefore lengthened and changed the value of the axial stretch without thickening its wall or growing inward or outward, thereby holding constant the values for wall thickness and inner and outer diameter and maintaining the levels of shear stress and circumferential stress on the vascular SMCs. Culturing the *mdx* and *sgcd-/-* mouse carotid arteries at axial stretch ratios different than the estimated *in vivo* value could elucidate the remodeling process that occurs in the absence of the DGC.

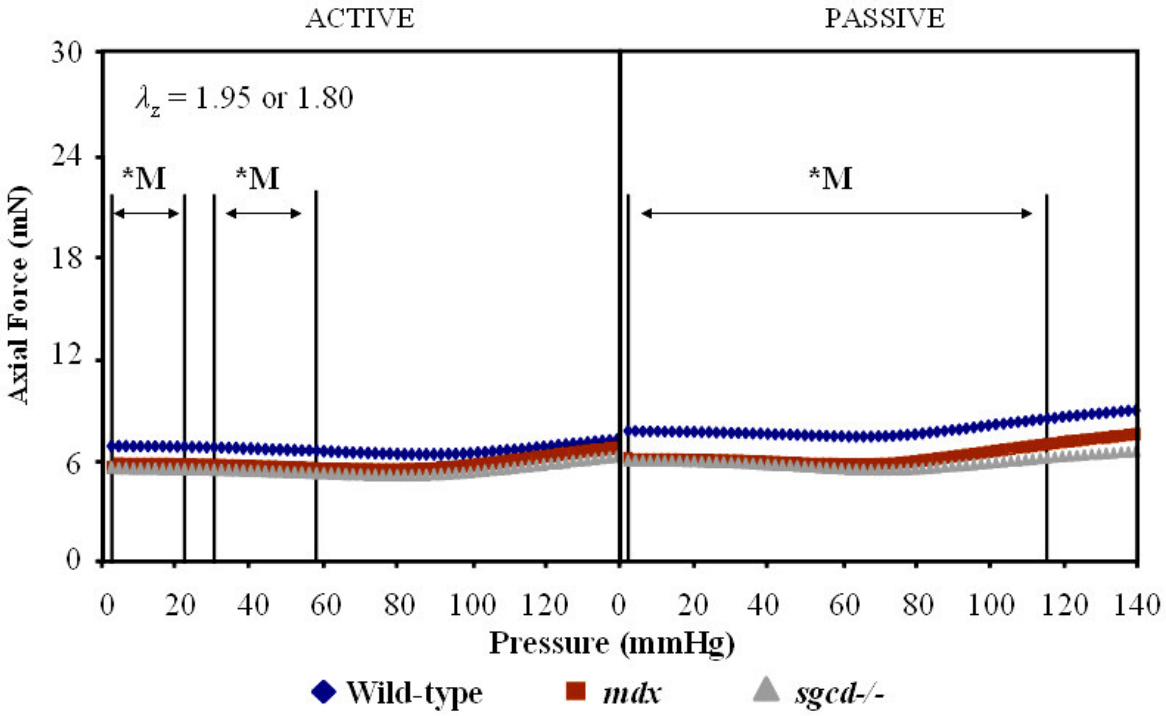

Figure 12: Active (basal tone) and passive (Ca^{2+} free) axial force for *P-d* curves at the high (λ_z = 1.95) axial stretch setpoint for the wild-type and at the mid (λ_z = 1.80) axial stretch setpoint for the *mdx* and *sgcd-/-* arteries. Comparing the results from these two different axial stretch setpoints allows us to see the change in diameter over pressurization for all three groups of vessels when stretched to ~1.05 of their *in vivo* axial stretch. The axial force values for the *sgcd-/-* are decreased but not significantly different from the wild-type in either the active or passive state ($p < 0.05$). *mdx* values are significantly decreased from the wild-type over low pressures in the active state and over a wide range of pressures (P = 2 – 116 mmHg) in the passive state (indicated by ***M→**).

It also is possible that changes in the cross-linking of the ECM occur in the absence of the DGC, decreasing the load the ECM bears and consequently increasing the load on the vascular SMCs. When α-dystroglycan, a component of the DGC, binds to laminin in the extracellular matrix, a mechanical link is formed. Further, this binding may induce laminin polymerization and formation of an organized extracellular network that leads to changes in cytoskeletal architecture[9]. Although $\alpha_7\beta_1$ integrins, as mentioned earlier, can replicate the mechanical link between laminin and muscle cell cytoskeletons, and are upregulated in *mdx* and *sgcd-/-* mice, they may not be able to compensate for the role of α-dystroglycan in initiating laminin binding and polymerization. As a result, the ECM will be weakened with the reduction in cross-linking, and axial stress on the vascular SMCs will be increased, thus causing growth and remodeling to a decreased *in vivo* axial stretch. Also, the actin reorganization and transmembrane signaling involved with the laminin polymerization process may be affected, causing altered mechanical properties of vascular SMCs that may cause a changed *in vivo* axial stretch ratio.

The results of our studies on the carotid arteries of mice lacking the genes that produce dystrophin or sarcoglycan-delta (proteins associated with human muscular dystrophies) show that the vascular system as well as the skeletal muscle is affected when these proteins are absent. Current muscular dystrophy research efforts are focused on providing a better and longer life for patients with muscular dystrophy. As DMD and other muscular dystrophy patients with better medical treatment live longer, there is concern that they may suffer from cardiovascular diseases such as hypertension and atherosclerosis that affect many aging Americans. They may require special medical treatment, though, if their vascular system has been altered in the absence of dystrophin or other DGC proteins. We have shown that the vascular systems of mice lacking an intact DGC undergo mechanical alterations, and smooth muscle cells that make up the vascular

system in humans with DMD and LGMD may also be subject to mechanical or structural changes. It is therefore constructive to continue to study the vasculature in the absence of dystrophin, sarcoglycan-delta, and other DGC components in order to understand how the vessel remodels to a new, functional state without the DGC. Understanding the mechanism of adaptation of blood vessels that lack the DGC should further our understanding of DMD and other muscular dystrophies, and may equip physicians to more effectively treat patients with these disorders.

CHAPTER III

CONCLUSIONS AND RECOMMENDATIONS

The results of our studies on the large arteries of mice lacking the genes that produce dystrophin or sarcoglycan-delta (proteins associated with human muscular dystrophies) show that the vascular system as well as the skeletal muscle is affected when these proteins are absent. Although at this point we can only speculate as to the mechanism for these mechanical differences in the vascular system, steps could be taken to obtain evidence to investigate some of our preliminary conclusions without conducting additional mechanical tests. First, we recommend that the tissue from the untested right carotid arteries or the mouse aortas be tested for content of relevant proteins such as utrophin and $\alpha_7\beta_1$ and $\alpha_5\beta_1$ integrins. The aortic segments from the three different mouse types have already been processed to be assayed on a micro-array, and those results may further guide us to test for additional pertinent proteins. Second, we recommend that the frozen sections of the tested left carotid arteries be stained for visualization of the $\alpha_7\beta_1$ and $\alpha_5\beta_1$ integrins, but also for the presence and location of fibronectin and laminin. Also, we recommend that the sections be analyzed to determine the dimensions, especially the wall-thickness, of cross-sections for the different mouse types as a verification of the results we gathered by measuring the arteries in the device. It may be possible, too, to analyze the sections for collagen mass-fraction using birefringence, and this analysis would provide another piece of information to help us discern the biomechanical process that has taken place in the *mdx* and *sgcd-/-* carotid arteries.

Once these tissue analyses have been conducted, we recommend testing of additional *mdx* and *sgcd-/-* arteries. One simple test that could be done is a measurement of the *in vivo* and *ex vivo* axial stretch ratio of the carotid arteries of all three types of mice. This could be done

crudely with calipers or more sophisticatedly with a computer-imaging system linked to a microscope. Although these measurements may not be a perfect reflection of the true *in vivo* axial stretch, as the surgery to visualize the arteries may introduce extra axial stretches, it could still lend evidence to either support or disprove our interpretation of the results. Another experiment that would be telling is culturing these arteries over a period of days to try to induce and measure vascular remodeling. Our results suggest that these arteries have remodeled significantly in response to increases in axial stress, and so it would be interesting to culture the arteries at increased and decreased axial stresses and observe the mechanical and molecular response. It would also be worthwhile to use the *in vivo* axial stretch values we inferred to set-up these arteries at conditions that accurately reflect their *in vivo* situation. Although our results did not show that these arteries had remodeled to adjust to circumferential or wall shear stresses, it is possible that the remodeling response of the arteries that lack an intact DGC to high pressure or high flow will be different than the normal response. In fact, previous acute studies have shown attenuated flow-induced dilation responses of *mdx* carotid arteries.[28,30] Culturing both *mdx* and *sgcd-/-* arteries for two or more days in high pressure or high flow culture conditions would enable us to record any altered mechanical adaptation that occurs in the knockout vessels under increased circumferential and shear stresses. For these future experiments, another method could be employed to assess any changes in the orientation of elastin in the ECM. En face confocal microscopy has been used to visualize the internal elastic laminae, the layers of extracellular matrix that are present between vascular SMCs in arteries. In this method (described by Jackson et al.[25]), vessels are opened longitudinally and mounted for examination with a confocal microscope, as the internal elastic laminae possess natural autofluorescence and allow visualization of elastin and fenestrae present between the layers of vascular SMCs.

These recommended experiments would contribute to current muscular dystrophy research efforts that are focused on providing a better and longer life for patients with muscular dystrophy. As DMD and other muscular dystrophy patients with better medical treatment live longer, there is concern that they may suffer from cardiovascular diseases such as hypertension and atherosclerosis that affect many aging Americans. They may require special medical treatment, though, if their vascular system has been altered in the absence of dystrophin or other DGC proteins. We have shown that the vascular systems of mice lacking an intact DGC undergo mechanical alterations, and smooth muscle cells that make up the vascular system in humans with DMD and LGMD may also be subject to mechanical or structural changes. It is therefore constructive to continue to study the vasculature in the absence of dystrophin, sarcoglycan-delta, and other DGC components in order to understand how the vessel remodels to a new, functional state without the DGC. As we further our understanding of the mechanism of adaptation of blood vessels that lack the DGC, this should further our understanding of DMD and other muscular dystrophies, as well as vascular growth and remodeling principles. We hope that through these findings, we may equip physicians to more effectively treat patients with these muscular dystrophies and vascular diseases.

REFERENCES

[1] Ahn, A. H., and L. M. Kunkel. Syntrophin binds to an alternatively spliced exon of dystrophin. *J. Cell Biol*. 128:363-371, 1995.

[2] Allikian, M. J., A. A. Hack, S. Mewborn, U. Meyer, and E. M. McNally. Genetic compensation for sarcoglycan loss by integrin alpha7beta1 in muscle. *J. Cell Sci*. 117:3821-3830, 2004.

[3] Blake, D. J., A. Weir, S. E. Newey, and K. E. Davies. Function and genetics of dystrophin and dystrophin-related proteins in muscle. *Physiol. Rev*. 92:291-329, 2002.

[4] Brenman, J. E., D. S. Chao, S. H. Gee, A. W. McGee, S. E. Craven, D. R. Santillano, Z. Wu, F. Huang, H. Xia, M. F. Peters, S. C. Froehner, and D. S. Bredt. Interaction of nitric oxide synthase with the postsynaptic density protein PSD-95 and alpha1-syntrophin mediated by PDZ domains. *Cell* 84:757-767, 1996.

[5] Byrne, E., A. J. Kornberg, and R. Kapsa. Duchenne muscular dystrophy: hopes for the sesquicentenary. *Med. J. Aust*. 179:463-464, 2003.

[6] Carnwarth, J. W. and D. M. Shotton. Muscular dystrophy in the mdx mouse: histopathology of the soleus and extensor digitorum longus muscles. *J. Neurol. Sci*. 80:39-54, 1987.

[7] Clerin, V., J. W. Nichol, M. Petko, R. J. Myung, J. W. Gaynor, and K. J. Gooch. Tissue engineering of arteries by directed remodeling of intact arterial segments. *Tissue Eng*. 9:461-472, 2003.

[8] Cohn, R. D. and K. P. Campbell. Molecular basis of muscular dystrophies. *Muscle Nerve* 23: 1456-1471, 2000.

[9] Colognato, H., D. A. Winkelmann, and P. D. Yurchenco. Laminin polymerization induces a receptor-cytoskeleton network. *J. Cell Bio.*145:619-631, 1999.

[10] Coral-Vazquez, R., R. D. Cohn, S. A. Moore, J. A. Hill, R. M. Weiss, R. L. Davisson, V. Straub, R. Barresi, D. Bansai, R. F. Hrstka, R. Williamson, and K. P. Campbell. Disruption of the sarcoglycan-sarcospan complex in vascular smooth muscle: a novel mechanism for cardiomyopathy and muscular dystrophy. *Cell* 98:465-474, 1999.

[11] Coulton, G. R., N. A. Curtin, J. E. Morgan, and T. A. Partridge. The mdx mouse skeletal muscle myopathy: II. Contractile properties. *Neuropathol. Appl. Neurobiol*. 14:299-314, 1998.

[12] Deconinck, A. E., J. A. Rafael, J. A. Skinner, S. C. Brown, A. C. Potter, L. Metzinger, D. J. Watt, J. G. Dickson, J. M. Tinsley, and K. E. Davies. Utrophin-dystrophin-deficient mice as a model for Duchenne muscular dystrophy. *Cell* 90:717-727, 1997.

[13] Dincer, P., Z. Akcoren, E. Demir, O. Sancak, G. Kale, S. Ozme, A. Karaduman, E. Tan, J. A. Urtizberea, J. S. Beckmann, and H. Topaloglu. A cross section of autosomal recessive limb-girdle muscular dystrophies in 38 families. *J. Med. Genet*. 37:361-367, 2000.

[14] Ervasti, J. M., and K. P. Campbell. A role for the dystrophin-glycoprotein complex as a transmembrane linker between laminin and actin. *J. Cell Bio*. 122:809-823, 1993.

[15] Gleason, R. L., Gray S. P., E. Wilson, and J. D. Humphrey. A multiaxial computer-controlled organ culture and biomechanical device for mouse carotid arteries. *J. Biomech. Eng*. 126:787-795*,* 2004.

[16] Gleason, R. L., E. Wilson, J. D. Humphrey. Biaxial biomechanical adaptations of mouse carotid arteries cultured at altered axial extension. Submitted to *J. Biomech*., 2004.

[17] Gleason, R. L. and J. D. Humphrey. Effects of a sustained extension on arterial growth and remodeling: a theoretical study. *J. Biomech*. 38:1255-1261, 2005.

[18] Goudemant, J. F., N. Deconinck, J. M. Tinsley, R. Demeure, A. Robert, K. E. Davies, and J. M. Gillis. Expression of truncated utrophin improves pH recovery in exercising muscles of dystrophic mdx mice: a 31P NMR study. *Neuromuscul. Disord.* 8:371-379, 1998.

[19] Gowers, W.R. Clinical lecture on pseudo-hypertrophic muscular paralysis. *Lancet* 2:1-2, 1879.

[20] Hack, A. A., M. J. Lam, L. Cordier, D. I. Shoturma, C. T. Ly, M. A. Hadhazy, M. R. Hadhazy, H. L. Sweeney, and E. M. McNally. Differential requirement for individual sarcoglycans and dystrophin in the assembly and function of the dystrophin-glycoprotein complex. *J. Cell Sci.* 113:2535-2544, 2000.

[21] Hayward, I. P., K. R. Bridle, G. R. Campbell, P. A. Underwood, and J. H. Campbell. Effect of extracellular matrix proteins on vascular smooth muscle phenotype. *Cell Biol. Int*. 19:727-734, 1995.

[22] Hodges, B. L., Y. K. Hayashi , I. Nonaka , W. Wang, K. Arahata, and S. J. Kaufman. Altered expression of the alpha7beta1 integrin in human and murine muscular dystrophies. *J. Cell Sci*. 110:2873-2881, 1997.

[23] Hoffman, E. P., R. H. Brown, Jr., and L. M. Kunkel. Dystrophin: the protein product of the Duchenne Muscular Dystrophy Locus. *Cel*l 51:919-928, 1987.

[24] Humphrey, J. D. Cardiovascular Solid Mechanics: Cells, Tissues and Organs. New York: Springer, 2002, pp. 18-24, 281.

[25] Jackson, Z. S., A. I. Gotlieb, and B. L. Langille. Wall tissue remodeling regulates longitudinal tension in arteries. *Circ. Res*. 90:918-925, 2002.

[26] Katoh, Y., and M. Periasamy. Growth and differentiation of smooth muscle cells during vascular development. *Trends Cardiovasc. Med*. 6:100-106, 1996.

[27] Khurana, T. S., S. C. Watkins, P. Chafey, J. Chelly, F. M. Tome, M. Fardeau, J. C. Kaplan, and J. M. Kunkel. Immunolocalization and developmental expression of dystrophin related protein in skeletal muscle. *Neuromuscul. Disord*. 1:185-194, 1991.

[28] Loufrani, L., K. Matrougui, D. Gorny, M. Duriez, I. Blanc, B. I. Levy, and D. Henrion. Flow (shear stress)–induced endothelium-dependent dilation is altered in mice lacking the gene encoding for dystrophin. *Circulation* 103:864-670, 2001.

[29] Loufrani, L., B. I. Levy, and D. Henrion. Defect in microvascular adaptation to chronic changes in blood flow in mice lacking the gene encoding for dystrophin. *Circ. Res*. 91:1183-1189, 2002.

[30] Loufrani, L., C. Dubroca, D. You, Z. Li, B. Levy, D. Paulin, and D. Henrion. Absence of dystrophin in mice reduced NO-dependent vascular function and vascular density: total recovery after a treatment with the aminoglycoside gentamicin. *Arterioscler. Thromb. Vasc. Biol*. 24:671-676, 2004.

[31] Matsumura, K., J. M. Ervasti, K. Ohlendieck, S. D. Kahl, and K. P. Campbell. Association of dystrophin-related protein with dystrophin-associated proteins in mdx mouse muscle. *Nature* 360:588-591, 1992.

[32] Mechler, F., F. L. Mastaglia, J. Haggith, and D. Gardner-Medwin. Adrenergic receptor responses of vascular smooth muscle in Becker dystrophy. A muscle blood flow study using the 133 Xe clearance method. *J. Neurol. Sci*. 46:291-302, 1980.

[33] Miike, T., S. Sugino, Y. Ohtani, K. Taku, and K. Yoshioka. Vascular endothelial cell injury and platelet embolism in Duchenne muscular dystrophy at the preclinical stage. *J. Neurol. Sci*. 82:67-80, 1987.

[34] Moiseeva, E. P. Adhesion receptors of vascular smooth muscle cells and their functions. *Cardiovasc. Res*. 52:372-386, 2001.

[35] Monaco, A. P., C. J. Bertelson, W. Middlesworth, C. Colletti, J. Aldridge, K. H. Fischbeck, R. Bartlett, M. A. Pericak-Vance, A. D. Roses, and L. M. Kunkel. Detection of deletions spanning the Duchenne muscular dystrophy locus using a tightly linked DNA segment. *Nature* 316:842-845, 1985.

[36] Noordeen, M. H., F. S. Haddad, F. Muntoni, P. Gobbi, J. S. Hollyer, and G. Bentley. Blood loss in Duchenne muscular dystrophy: vascular smooth muscle dysfunction? *J. Pediatr. Orthop.* B. 8:212-215, 1999.

[37] Ozawa, E., S. Noguchi, Y. Mizuno, Y. Hagiwara, and M. Yoshida. From dystrophinopathy to sarcoglycanopathy: evolution of a concept of muscular dystrophy. *Muscle Nerve* 21:421-438, 1998.

[38] Pasternak, C., S. Wong, and E. L. Elson. Mechanical function of dystrophin in muscle cells. *J. Cell Biol*. 128:355-361, 1995.

[39] Pastoret, C., and A. Sebille. Further aspects of muscular dystrophy in mdx mice. *Neuromusc. Disord*. 3:470-475, 1993.

[40] Pastoret, C. and A. Sebille. mdx mice show progressive weakness and muscle deterioration with age. *J. Neurol. Sci*. 129:97-105, 1995.

[41] Petrof, B. J., J. B. Shrager, H. H Stedman, A. M. Kelly, and H. L. Sweeney. Dystrophin protects the sarcolemma from stresses developed during muscle contraction. *Proc. Natl. Acad. Sci. U.S.A*. 90:3710-3714, 1993.

[42] Petrof, B. J. The molecular basis of activity-induced muscle injury in Duchenne muscular dystrophy. *Mol. Cell. Biochem*. 179:111-123, 1998.

[43] Reitter, B. and H. H. Goebel. Dystrophinopathies. *Semin. Pediatr. Neurol.* 3:99-109, 1996.

[44] Sciandra, F., M. Bozzi, M. Bianchi, E. Pavoni, B. Giardina and A. Brancaccio. Dystroglycan and muscular dystrophies related to the dystrophin-glycoprotein complex. *Ann. 1st Super Sanita* 39:173-181, 2003.

[45] Sicinski, P., Y. Geng, A. S. Ryder-Cook, E. A. Barnard, M. G. Darlison, and P. J. Barnard. The molecular basis of muscular dystrophy in the mdx mouse: a point mutation. *Science* 244:1578-1580, 1989.

[46] Stenmark, K.R. and R.P. Mecham. Cellular and molecular mechanisms of pulmonary vascular remodeling. *Annu. Rev. Physiol*. 59:89-144, 1997.

[47] Thomas, G. D., P. W. Shaul, I. S. Yuhanna, S. C. Froehner, and M. E. Adams. Vasomodulation by skeletal muscle-derived nitric oxide requires alpha-syntrophin-mediated sarcolemmal localization of neuronal nitric oxide synthase. *Circ. Res*. 92:554-560, 2003.

[48] Thyberg, J., K. Blomgren, J. Roy, P. K. Tran, and U. Hedin. Phenotypic modulation of smooth muscle cells after arterial injury is associated with changes in the distribution of laminin and fibronectin. *J. Histochem. Cytochem*. 45:837-846, 1997.

[49] Tinsley, J. M., D. J. Blake, A. Roche, U. Fairbrother, J. Riss, B. C. Byth, A. E. Knight, J. Kendrick-Jones, G. K. Suthers, D. R. Love, and Y. H. Edwards. Primary structure of dystrophin-related protein. *Nature* 360:591-593, 1992.

[50] Tyler, K. L. Origins and early descriptions of "Duchenne muscular dystrophy". *Muscle Nerve* 28:402-422, 2003.

[51] Vaishnav, R.N., J. Vossoughi, D.J. Patel, L.N. Cothran, B.R. Coleman, and E.L. Ison-Franklin. Effect of hypertension and elasticity and geometry of aortic tissue from dogs. *J. Biomech. Engr.* 112:70-74, 1990.

[52] Walton, J. N. and F. J. Nattrass. On the classification, natural history and treatment of the myopathies. *Brain* 77:169-231, 1954.

[53] Yoshida, M., A. Suzuki, H. Yamamoto, S. Noguchi, Y. Mizuno, and E. Ozawa. Dissociation of the complex of dystrophin and its associated proteins into several unique gropus by n-octyl beta-D-glucoside. *Eur. J. Biochem.* 222:1055-1061, 1994.

APPENDIX

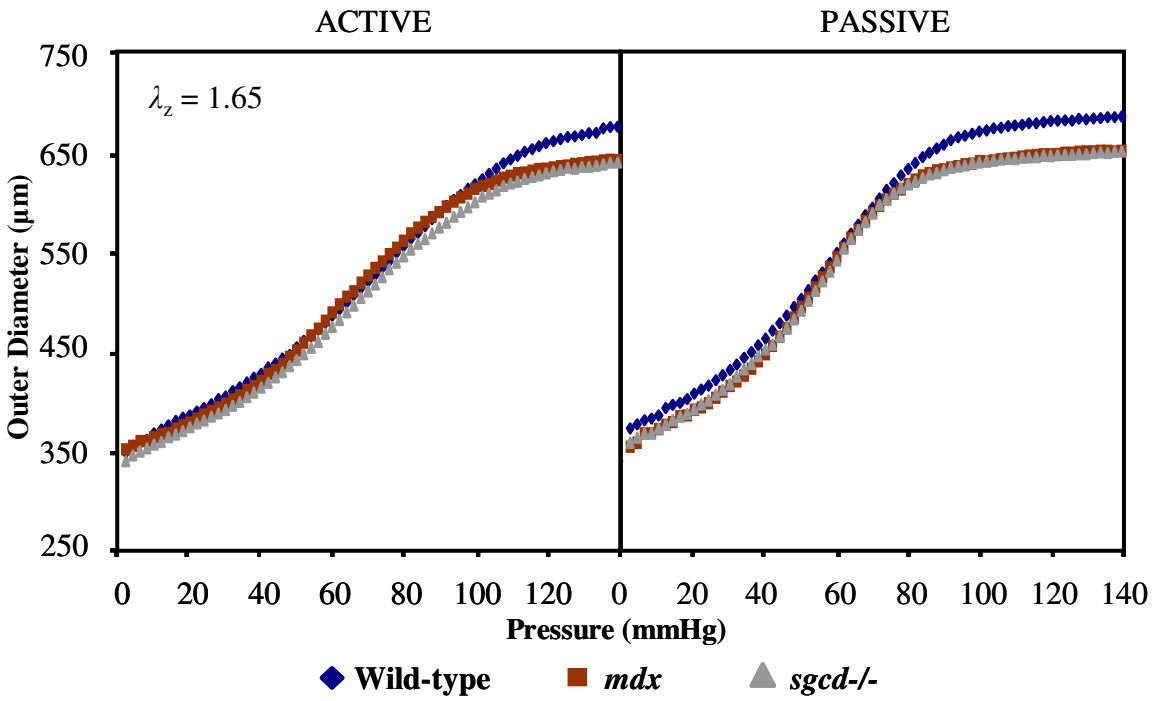

Figure 13: Active (basal tone) and passive (Ca^{2+} free) *P-d* curves at the low (λ_z = 1.65) axial stretch setpoint. The mdx and sgcd-/- curves tend to diverge from the wild-type at high pressures in the active state, but at lower pressures in the passive state. Although trends are visible, there were no significant differences ($p < 0.05$) for this data.

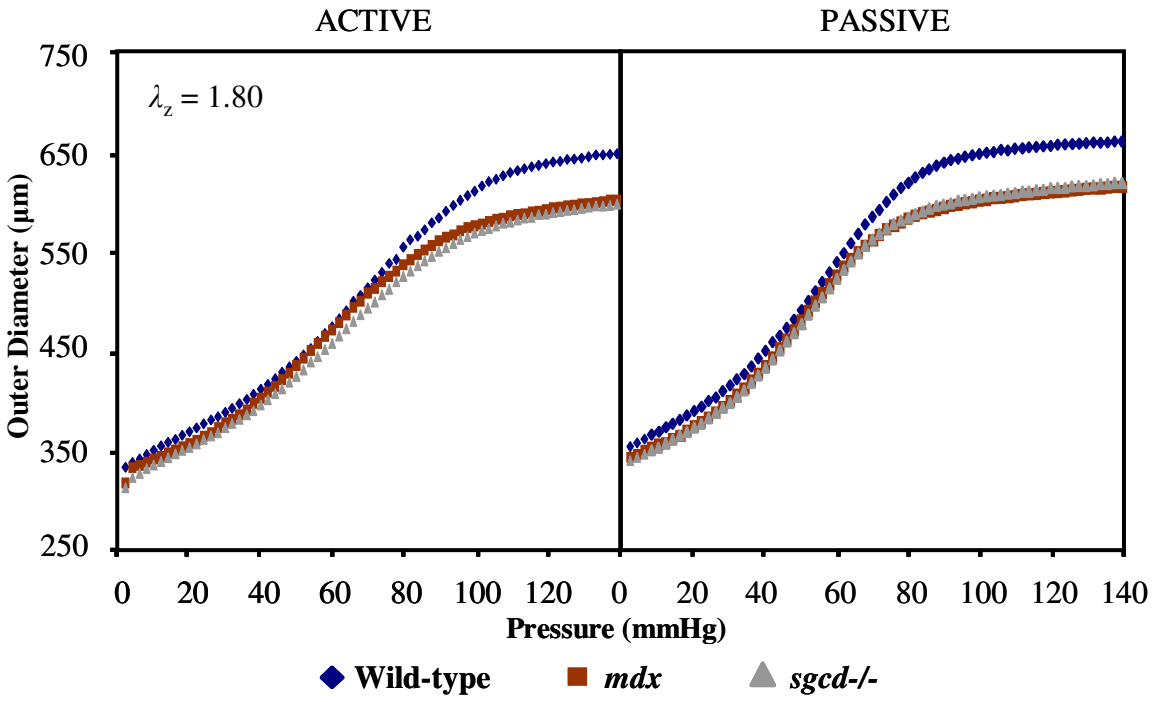

Figure 14: Active (basal tone) and passive (Ca^{2+} free) *P-d* curves at the mid (λ_z = 1.80) axial stretch setpoint. The *mdx* and *sgcd-/-* curves tend to diverge from the wild-type at mid-range pressures in both the active and passive states, although there were no significant differences ($p < 0.05$) for this data.

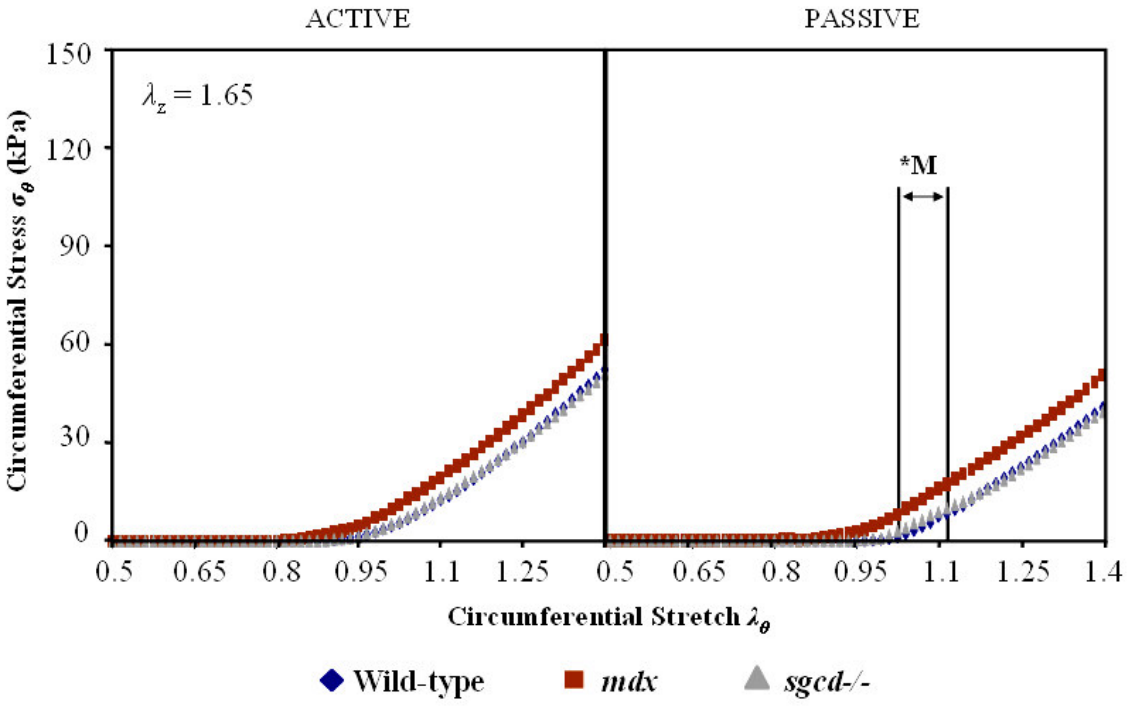

Figure 15: Active (basal tone) and passive (Ca^{2+} free) circumferential stress-stretch curves at the low (λ_z = 1.65) axial stretch setpoint. There was a range of circumferential stretch values (λ_θ = 1.01 – 1.115) in the passive state, indicated by ***M**, for which the *mdx* circumferential stresses were significantly greater (p < 0.05) than the wild-type values.

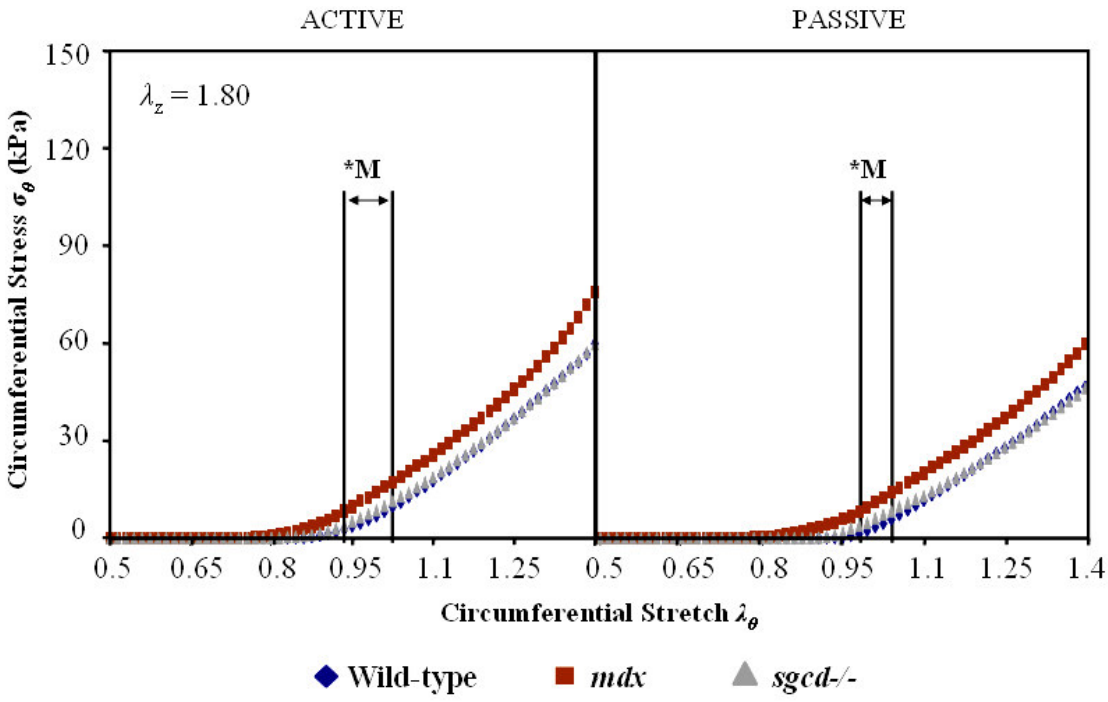

Figure 16: Active (basal tone) and passive (Ca^{2+} free) circumferential stress-stretch curves at the mid (λ_z = 1.80) axial stretch setpoint. There was a range of circumferential stretch values (λ_θ = 0.935 – 1.025) in the active state and (λ_θ = 0.980 – 0.140) in the passive state, indicated by ***M,** for which the *mdx* circumferential stresses were significantly greater ($p < 0.05$) than the wild-type values.

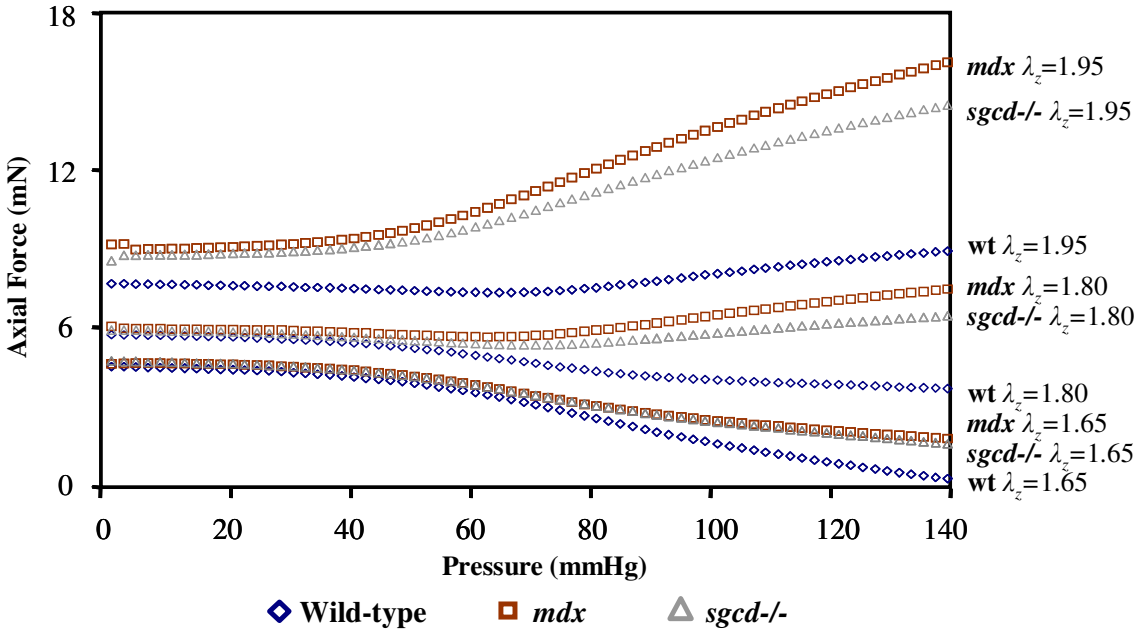

Figure 17: Passive axial force response during *P-d* test for all mouse types at all axial stretch setpoints. Mouse type (wt = wild-type) and axial stretch are indicated on the right axis where the curve ends. Note the disparity between the wild-type and knockout curves at the high axial stretch and the relative similarity between the wild-type curve at the high axial stretch (λ_z =1.95) and the *mdx* and *sgcd-/-* curves at the mid axial stretch (λ_z =1.8), just as we saw in the active axial force response.

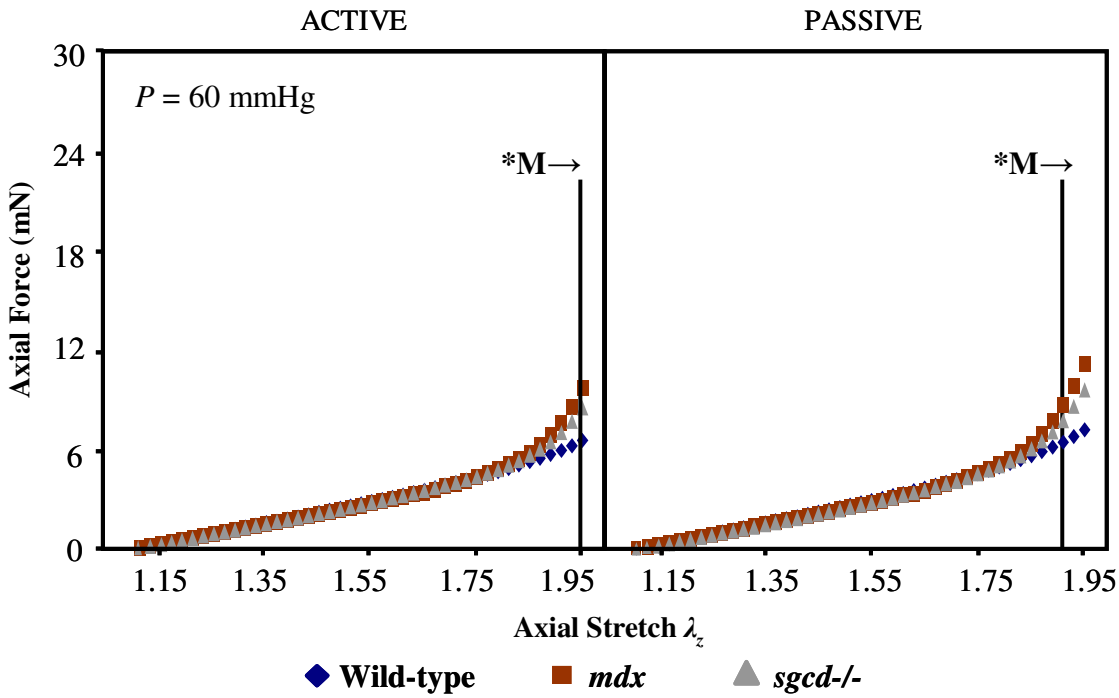

Figure 18: Active (basal tone) and passive (Ca^{2+} free) axial *f-ℓ* curves at the low (P = 60 mmHg) pressure setpoint. Note that the axial force for the *mdx* and *sgcd-/-* tend to be greater than the wild-type at the higher axial stretches. The *mdx* values become significantly different ($p < 0.05$) from the wild-type at the axial stretch λ_z = 1.95 in the active state and at λ_z = 1.91 – 1.95 in the passive state (indicated by the ***M→**). The *sgcd-/-* values are significantly different for the pressure range λ_z = 1.81 – 1.95 in the active state and λ_z = 1.77 – 1.95 in the passive state (indicated by the ***S→**).

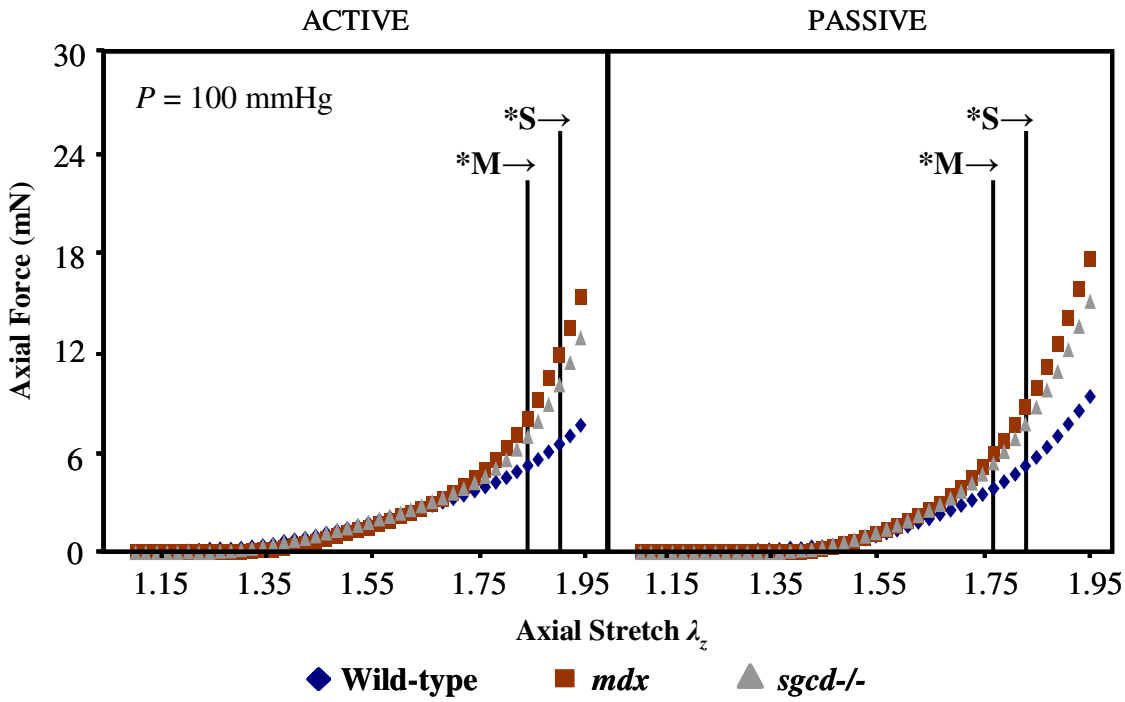

Figure 19: Active (basal tone) and passive (Ca^{2+} free) axial *f*-ℓ curves at the mid (P = 100 mmHg) pressure setpoint. Note that the axial force for the *mdx* and *sgcd-/-* tend to be greater than the wild-type. The *mdx* values become significantly different ($p < 0.05$) from the wild-type over the axial stretch range λ_z = 1.85 – 1.95 in the active state and at λ_z = 1.77 – 1.95 in the passive state (indicated by the ***M→**). The *sgcd-/-* values are significantly different for the pressure range λ_z = 1.91 – 1.95 in the active state and λ_z = 1.83 – 1.95 in the passive state (indicated by the ***S→**).

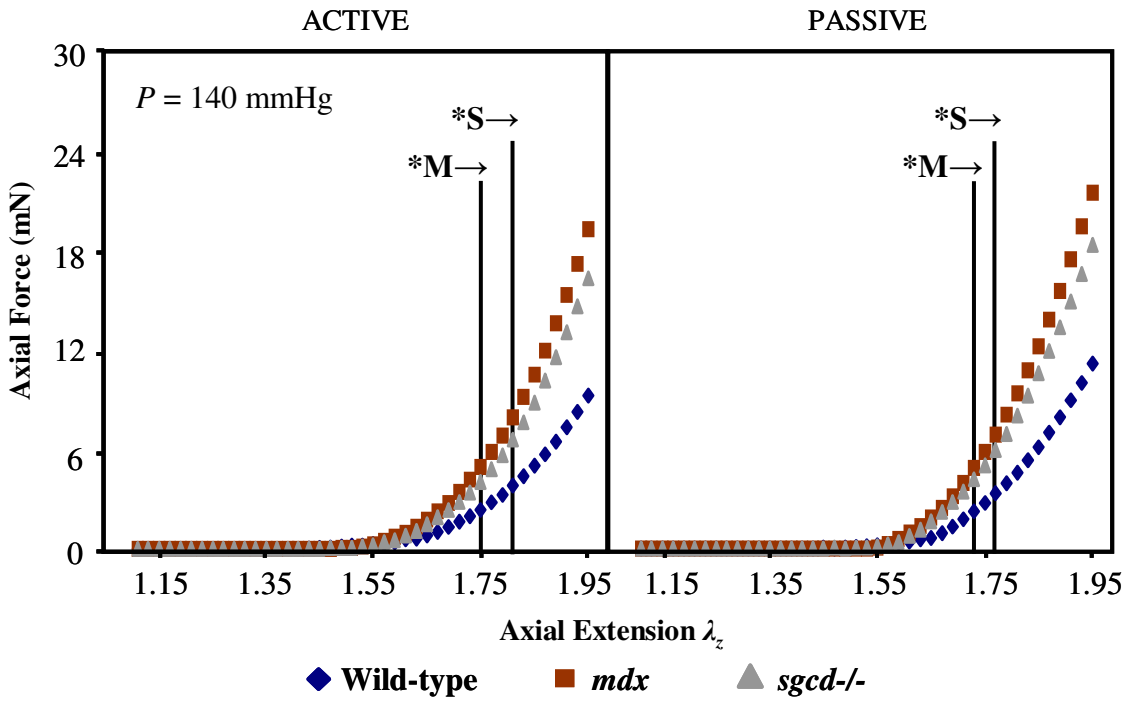

Figure 20: Active (basal tone) and passive (Ca^{2+} free) axial *f*-ℓ curves at the high (P = 140 mmHg) pressure setpoint. Note that the axial force for the *mdx* and *sgcd-/-* are clearly greater than the wild-type. The *mdx* values become significantly different ($p < 0.05$) from the wild-type over the axial stretch range λ_z = 1.75 – 1.95 in the active state and at λ_z = 1.73 – 1.95 in the passive state (indicated by the ***M→**). The *sgcd-/-* values are significantly different for the pressure range λ_z = 1.81 – 1.95 in the active state and λ_z = 1.77 – 1.95 in the passive state (indicated by the ***S→**).

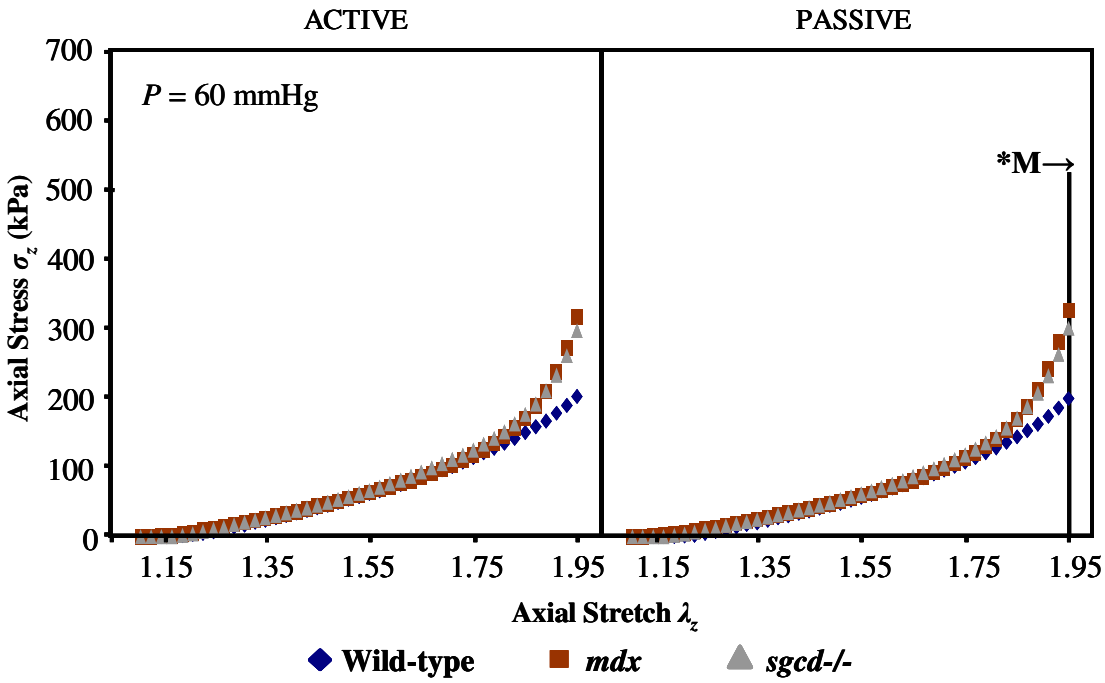

Figure 21: Active (basal tone) and passive (Ca^{2+} free) axial stress-stretch curves at the low (P = 60 mmHg) pressure setpoint. There were no significant differences in the active state. The *mdx* values become significantly different ($p < 0.05$) from the wild-type at the axial stretch $\lambda_z = 1.95$ in the passive state (indicated by the ***M→**).

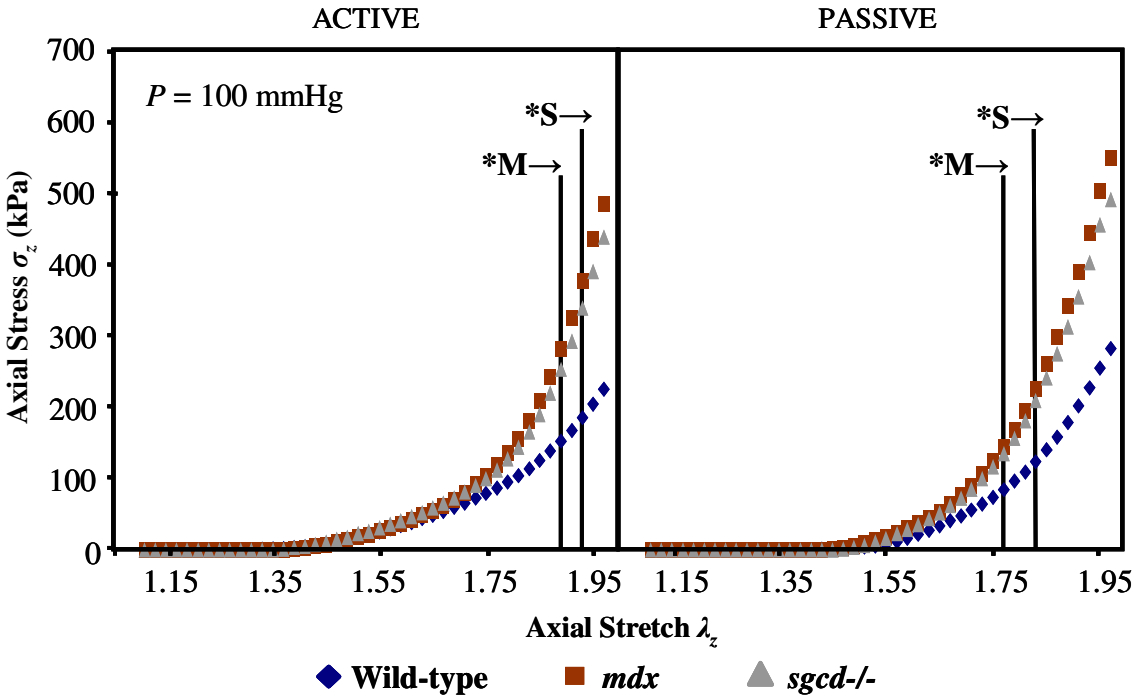

Figure 22: Active (basal tone) and passive (Ca^{2+} free) axial stress-stretch curves at the mid (P = 100 mmHg) pressure setpoint. The axial stresses for the *mdx* and *sgcd-/-* tend to be greater than the wild-type in both the active and passive state, but the significant differences are more evident in the passive state. The *mdx* values become significantly different ($p < 0.05$) from the wild-type over the axial extension range λ_z = 1.89 – 1.95 in the active state and at λ_z = 1.77 – 1.97 in the passive state (indicated by the ***M→**). The *sgcd-/-* values are significantly different for the pressure range λ_z = 1.93 – 1.97 in the active state and λ_z = 1.83 – 1.97 in the passive state (indicated by the ***S→**).

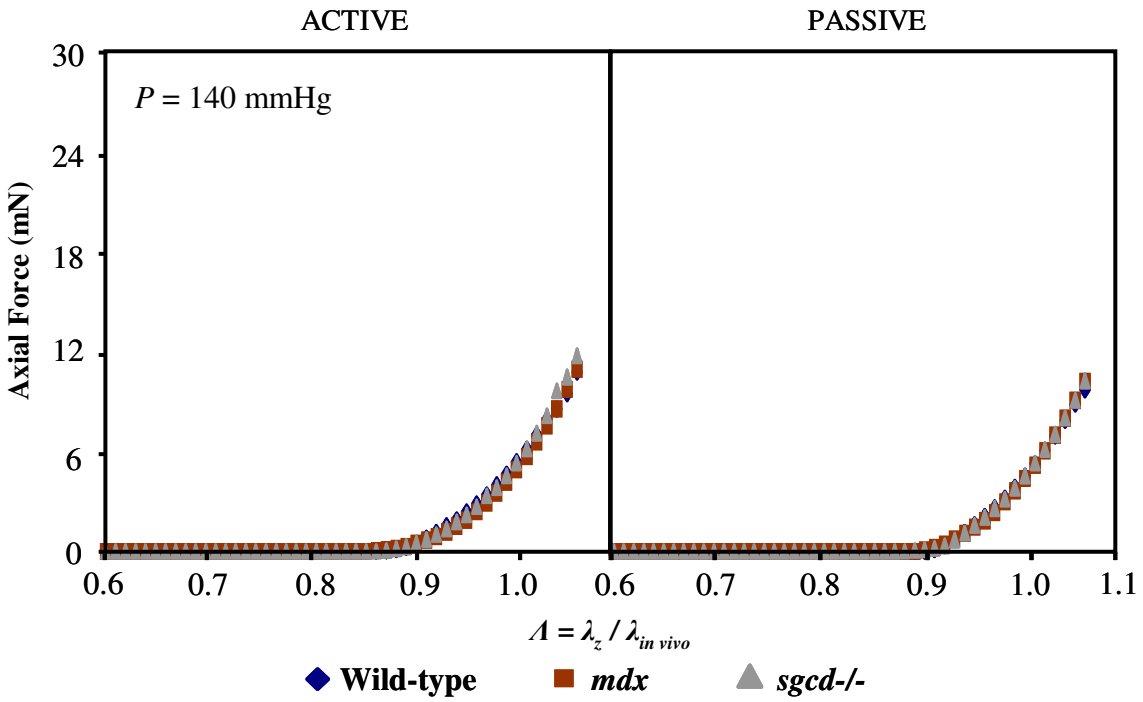

Figure 23: Active (basal tone) and passive (Ca^{2+} free) axial *f*-ℓcurves, with the axial stretch normalized to the *in vivo* axial stretch, at the high (*P* = 140mmHg) pressure setpoint. The axial force values for the *mdx* and *sgcd-/-* are no longer significantly different from the wild-type in either the active and passive state ($p < 0.05$) when the axial stretch is normalized to the estimated *in vivo* axial stretch for each mouse type.

VITA

WENDY WATSON DYE
Department of Biomedical Engineering
337 Zachry Engineering Center, 3120 TAMU
College Station, TX 77843-3120
Email: wendy.dye@gmail.com

EDUCATION
Texas A&M University (TAMU), College Station, TX

- Master of Science, Biomedical Engineering, GPR 3.850 / 4.0, August 2005
- Bachelor of Science, Biomedical Engineering, GPR 3.779/ 4.0 (*magna cum laude*), December 2003

RESEARCH EXPERIENCE
Research Internship with RUBI Program (Research for Undergraduates in Biomechanics and Imaging) at University of Rochester, Rochester NY, 40 hrs/wk, Summer 2002

- Cell culture and observation through time-lapse microscopy to assess wound healing
- Exposure to immunofluourescence techniques, establishment of protocol
- Participation in poster session

Graduate Assistant: TAMU Biomedical Engineering Deptartment, 2004–2005
Undergraduate Research Assistant: TAMU Biomedical Engineering Department, 2002–2003

- Set-up of organ culture device
- Froze/sectioned arteries, performed digital imaging of stained sections

INTERNATIONAL EXPERIENCE
Cultural exchange program in Uzbekistan, Summer 2003
Study Abroad Program to Paris, France with TAMU College of Engineering, Summer 2001

- 6 hours engineering course credit earned

ACADEMIC HONORS

- 2nd Prize in Bioengineering Oral Presentation Division, TAMU Student Research Week, 2005
- TAMU Graduate Merit Fellowship, 2004-2005, $30,000
- TAMU President's Endowed, Director's Excellence, and National Merit Scholarships; 2000–2004, $24,000
- 2nd Place in TRI-hard Triathlon Challenge (18-22 age group), Burnet TX, 2003
- TAMU Engineering Scholars Program: Selective program for engineering students designed to broaden their education and prepare them for a career in industry or academia
- TAMU E-zip Program: Unique fast-track program allowing engineering students to receive both bachelor's and master's degrees in 4-5 years by utilizing dual-degree credits for classes

ACTIVITIES
Tau Beta Pi, the Engineering Honor Society

- *Candidate Chair*, 2003–2004; *Fundraising Chair*, 2003

Half-marathon finisher, Austin TX, 2003
SWE (Society of Women Engineers)
Small group Bible study leader, 2001-2004